A unified solution to the small scale problems of the ΛCDM model II: introducing parent-satellite interaction

Antonino del Popolo, Morgan Le Delliou

Prepared for submission to JCAP

A unified solution to the small scale problems of the ΛCDM model II: introducing parent-satellite interaction

A. Del Popolo,[a,b] **M. Le Delliou**[c]

[a]Dipartimento di Fisica e Astronomia, University Of Catania, Viale Andrea Doria 6, 95125 Catania, Italy

[b]International Institute of Physics, Universidade Federal do Rio Grande do Norte, 59012-970 Natal, Brazil

[c]Instituto de Fisica Teorica IFT-UNESP, Rua Dr. Bento Teobaldo Ferraz 271, Bloco 2 - Barra Funda, 01140-070 São Paulo, SP Brazil

E-mail: adelpopolo@oact.inaf.it, delliou@ift.unesp.br

Abstract. We **continue the study of the impact from** baryon physics on the small scale problems of the ΛCDM model**, based on a semi-analytical model (Del Popolo, 2009). With such model, we show how the cusp/core, missing satellite (MSP), Too Big to Fail (TBTF) problems** and the angular momentum catastrophe can be reconciled with observations**, adding parent-sattelite interaction. Such interaction** between dark matter (DM) and baryons through dynamical friction (DF) can **sufficiently** flatten the inner cusp of the density profiles to solve the cusp/core problem. **Combining, in our model, a Zolotov et al. (2012)-like correction, similarly to Brooks et al. (2013), and effects of UV heating and tidal stripping, the number of massive, luminous satellites, as seen in the Via Lactea 2 (VL2) subhaloes,** is in agreement with the numbers observed in the MW, thus resolving the MSP and TBTF problems. The model also produces **a distribution of the angular spin parameter and angular momentum in agreement with observations of the dwarfs studied by van den Bosch, Burkert, & Swaters (2001).**

Keywords: cosmology: theory - large scale structure of universe - galaxies: formation

Contents

1 Introduction **1**

2 Solving the small scale problems of ΛCDM **6**
2.1 First phase: density profile flattening and CCP 7
2.2 Second phase: mass lost caused by tidal stripping and tidal heating 11
2.3 Evaluation of luminous satellites 14

3 Results and discussion **17**

4 Conclusions **22**

A Core formation model **28**

B Dynamics of the satellites. **31**
B.1 Dynamical friction 32
B.2 Mass loss 33
B.3 Tidal Heating 34

1 Introduction

The ΛCDM (cosmological constant and Cold Dark Matter) model of cosmology, although highly successful in describing the observations of the Universe, its large scale structure and evolution (Spergel et al. 2003, Komatsu et al. 2011; Del Popolo 2013, **2014a**), retains some problems in describing structures at small scales (e.g., Moore 1994; Moore et al. 1999; Ostriker & Steinhardt 2003; Boylan-Kolchin, Bullock, and Kaplinghat 2011, 2012; Oh et al. 2011)[1]. These are a) the cusp/core problem (hereafter CCP) (Moore 1994; Flores & Primak 1994), i.e. the discrepancy between the cuspy density profiles obtained in N-body simulations (Navarro, Frenk & White 1996, 1997; Navarro 2010) and the flat density profiles of dwarf **and Low Surface Brightness galaxies (LSBs)** (Burkert 1995; de Blok, Bosma, & McGauch 2003; Del Popolo 2009 (DP09), Del Popolo 2012a,b (DP12a, DP12b); Oh et al. 2010, 2011; Kuzio de Naray & Kaufmann 2011); b) the angular momentum catastrophe (AMC, van den Bosch, Burkert,& Swaters, 2001), that is the discrepancy between the large discs of observed spirals and the small discs obtained in Smooth Particle Hydrodynamics (SPH) simulations; c) the "missing satellite problem" (MSP), namely the discrepancy between the number of predicted and observed subhaloes when running N-body simulations (Klypin et al. 1999; Moore et al. 1999)[2].

This work extends a previous paper (Del Popolo *et al.* 2014), enriched with the part of the model described in appendix B, and will chiefly focus on the latter problem **(MSP). However**, the model also carry the solution for former two **(CCP and AMC)**, from the part of the model developed in Del Popolo *et al.* (2014) and summarized in appendix A. **In**

[1] Other remaining problems for the ΛCDM model involve understanding dark energy: the cosmological constant fine tuning problem (Weinberg 1989; Astashenok, & Del Popolo 2012), and the "cosmic coincidence problem".

[2] That difference is larger than an order of magnitude in the Milky Way (MW)!

clear, it uses a semi-analytical model to account for the dynamical evolution of satellites.

If the first author was one of the early promoters of the role of baryons, many author continue stressing this role (e.g. Governato *et al.*,2010; Macció *et al.*,2011; El-Zant *et al.*,2001,2004; Romano-Diaz *et al.*, 2008,2009; Cole *et al.*,2011; Inoue and Saitoh, 2011; Brooks *et al.*, 2013; Madau, Shen and Governato, 2014). More recently Governato *et al.* (2014), looking at faint dwarves, concluded that their results highlighted the importance of baryon physics for simulations, while Di Cintio *et al.* (2014) showed baryons flatten cusps in a wide mass range, a result almost identical to Del Popolo 2010 (DP10).

The model used in this work originated in DP09, where the results made famous in Governato *et al.* (2010) were originally published. Capable of handling the baryonic processes shaping the inner structure of clusters (and galaxies), it was able to predict the correct shape of the density profiles of clusters (DP12a; Del Popolo 2014a) and galaxies (DP09; Del Popolo & Kroupa 2009; DP12b), and correlations among several quantities in clusters of galaxies (DP12a; Del Popolo 2014b) later observed in Newman et al. (2013a,b), and so before the results from SPH simulations (e.g., Governato et al. 2010, 2012; Martizzi et al. 2012). Furthermore, dependence on the halo mass of inner density profiles slope was correctly predicted (DP10; Del Popolo 2011 (DP11)) while only later seen in SPH simulations of Di Cintio et al. (2013, 2014). Most recently, Polisensky and Ricotti (2014) compared their simulations to DP09 and DP10 finding them in perfect agreement with the predictions in those papers. Finally, Del Popolo & Hiotelis (2014) compared also the result of adding SF to the model with SPH simulations of Inoue & Saitoh (2011), finding agreement, while Del Popolo (2014a) showed that the effect of baryonic clumps exchanging energy and angular momentum with DM, for $V_{rot} \lesssim 40km/s$, is more effective in transforming cusps into cores than the effect of SF.

Klypin et al. (1999), and Moore et al. (1999) noticed that numerical simulations of galactic and cluster haloes predicted much more subhaloes than observed. They had found $\simeq 500$ satellites with circular velocities larger than Ursa-Minor and Draco, while the MW **dwarf Spheroidals (dSphs)** are well known to be far fewer (9 bright dSphs (Boylan-Kolchin, Bullock, and Kaplinghat 2012), Sagittarius, the **Large Magellanic Clouds – LMC – and the Small Magellanic Clouds – SMC**). The problem was later confirmed by other cosmological simulations (Aquarius, Via Lactea II (VL2), and GHALO simulations – Springel et al. 2008; Stadel et al. 2009; Diemand et al. 2007). It was alleviated with the discovery of the ultra-faint MW satellites (Willman et al. 2005; Belokurov 2006; Zucker 2006; Sakamoto & Hasegawa 2006; Irwin et al. 2007) but insufficiently for a complete solution.

Similarly to the solutions to other small scale problems, the resolution of the MSP can be distinguished into cosmological and astrophysical solutions. Cosmological solutions are based on the modification of the power spectrum at small scales (e.g. Zentner &Bullock 2003), or that of the constituent DM particles (Colin, Avila-Reese & Valenzuela 2000; Sommer-Larsen & Dolgov 2001; Hu, Barkana & Gruzinov 2000; Goodman 2000; Peebles 2000; Kaplinghat, Knox, & Turner, M. S. 2000). **Modified** gravity theories, like $f(R)$ (Buchdal 1970; Starobinsky 1980), $f(T)$ (see Ferraro 2012), and MOND (Milgrom 1983a,b), can **also** solve the problem.

Several different kinds of astrophysical solutions have been proposed. In one picture,

the present-day dwarf galaxies could have been more massive in the past, and they were transformed and reduced to their present masses by strong tidal stripping (e.g., Kravtsov, Gnedin & Klypin 2004). **Another** very popular picture is based on suppression of star formation due to supernova feedback (SF), photoionization (Okamoto et al. 2008; B13), and reionization. In particular, reionization can prevent the acquisition of gas by DM haloes of small mass, then "quenching" star formation after $z \simeq 10$ (Bullock, Kravtsov, & Weinberg 2000; Ricotti & Gnedin 2005; Moore et al. 2006). This would suppress dwarfs (dSphs) formation or could make them invisible. Another solution combines the change of central density profiles of satellites from cuspy to cored (Zolotov et al. 2012 (Z12); Brooks et al. 2013 (B13)), which makes the satellites more subject to tidal stripping and even subject to being destroyed (Strigari et al. 2007; Peñarrubia et al. 2010 (P10)). Tidal stripping is enhanced if the host halo has a disc. Disc shocking due to the satellites passing through the disc produce strong tidal effects on the satellites, **even** stronger **if** the satellite has a cored inner profile. The astrophysical solutions based on the role of baryons in structure formation, are more easy to constrain than cosmological solutions, and moreover do not request one to reject the ΛCDM **paradigm**.

The MSP has recently **enriched with** an extra problem, **spawned from** the analysis of the Aquarius and the Via Lactea simulations. Simulated haloes produced $\simeq 10$ subhaloes (Boylan-Kolchin, Bullock, and Kaplinghat 2011, 2012) that were too massive and dense to be the host of the MW brightest satellites: while those ΛCDM simulations predicted in excess of 10 subhaloes with $V_{max} > 25$ km/s, the dSphs of the MW all have $12 < V_{max} < 25$ km/s**. This** discrepancy in the **kinematics** between simulations and the MW brightest dSphs (Boylan-Kolchin, Bullock, and Kaplinghat 2011, 2012)**, an extra problem of the MSP,** has been dubbed the Too-Big-To-fail (TBTF) problem[3].

While it is not complicated to separately solve the MSP problem, and the TBTF problem with the **recipes discussed above**, a simultaneous solution of both problems in models of galaxy formation based on DM-only simulations of the ΛCDM model (Boylan-Kolchin, Bullock & Kaplinghat 2012)[4], is much more complicated.

Previous attempts to find a simultaneous solution to the abundance problem of satellites (MSP), and to the TBTF problem were made by the above mentioned Z12, and B13. Z12 found a correction to the velocity in the central kpc of galaxies, $\Delta v_{\rm c,1kpc}$, that mimicked the flattening of the cusp due to SF and tidal stripping.

This **correction,** together with its subsequent destruction effects from the tidal field of the baryonic disc, and the identification of subhaloes that remain dark because of **their** inefficiency in forming stars due to UV heating, were then applied by B13 to the subhaloes of the VL2 simulation (Diemand et al. 2008). As a result, the number of massive subhaloes in the VL2 were brought in line with the number of satellites of MW and M31.

The CCP emerges from the inner cuspy profiles predicted by different numerical simulations: defining the inner profile as $\rho \propto r^{\alpha}$, **simulations fit either a value $\alpha = -1$, in the case of the Navarro, Frenk, & White (1996, 1997) (hereafter NFW) profile, $\alpha = -1.5$, in the Moore et al (1998), and Fukushige & Makino (2001) simulations, or different values correlated to the objects considered (Jing & Suto 2000; Ricotti**

[3] "Too big to fail", in the sense that the extra simulation satellites are too big, compared with MW satellites, to remain invisible.

[4] **Note that, in the case of the TBTF problem,** the excess of massive subhaloes in MW could disappear if satellites density profiles are modeled through Einasto's profiles, or if the MW's virial mass is $\simeq 8 \times 10^{11} M_{\odot}$ instead of $\simeq 10^{12} M_{\odot}$ (Vera-Ciro et al. 2012; Di Cintio et al. 2013).

2003; Ricotti & Wilkinson, 2004; Ricotti Pontzen, & Viel 2007; DP10, DP11; Del Popolo, Cardone, & Belvedere 2013), from dwarf galaxies to clusters of galaxies. More recently, (Stadel et al. 2009; Navarro et al. 2010) have shown the Einasto profile to better fit density profiles. It is characterized by a profile increasingly flattening (becoming shallower) toward the center of the structure, until $\alpha \simeq 0.8$ at 120 pc (Stadel et al. 2009). This is the smallest slope obtained in simulations, but remains larger than in observations, as **galaxy inner density profiles are usually** flat or almost flat (Burkert 1995; de Blok, Bosma, & McGauch 2003; Swaters et al. 2003; Del Popolo 2009 (DP09) , Del Popolo 2012a,b (DP12a, DP12b); Del Popolo & Hiotelis 2014; Oh et al. 2011; Oh et al. 2010, 2011; Kuzio de Naray & Kaufmann 2011). Initially noticed in galaxies, **the CCP is also present for** clusters of galaxies. Flat inner density profiles were found in several clusters by Sand et al. (2004), and more recently in Newman et al. (2009, 2011, 2013).

Several solutions have already been proposed (see de Blok 2010 for a review). They can also be distinguished into cosmological and astrophysical **ones**. Cosmological solutions are similar to those for the MSP.

Astrophysical solutions stem from some "heating" mechanism inducing expansion of the DM component so that the resulting inner density is reduced. The **mechanisms proposed** are split in two categories: "supernova-driven flattening" (Navarro et al. 1996; Gelato & Sommer-Larsen 1999; Read & Gilmore 2005; Mashchenko et al. 2006, 2008; Governato et al. 2010; Pontzen & Governato 2011) or dynamical friction from baryonic clumps (El-Zant et al. 2001, 2004; Romano-Diaz et al. 2008, 2009; Del Popolo 2009; Cole et al. 2011). **The nature and size of those clumps, predicted in the ΛCDM model, has been discussed in many papers, including e.g. Inoue & Saitoh (2011) and Del Popolo** *et al.* **(2014). Such clumps are discussed, in Inoue & Saitoh (2011), as possible sources to form galactic bulges, change the DM density profile and induce significant stellar vs. galactic disk rotation. Del Popolo** *et al.* **(2014) provides an estimate of the mass of those clumps around 1% of the parent, but signals the possibility for micro haloes in ΛCDM, together with references of corroborating observations. There the similarity of mechanisms to flatten cores of the model with Inoue & Saitoh (2011) is pointed out.**

The "angular momentum catastrophe" appears in SPH simulations of galaxies: **those simulations show that the collapse does not conserve baryons' angular momentum: they only carry 10% of the angular momentum typical of real galaxies. However,** SPH disks are too small compared with real disks (Navarro & Benz 1991; Navarro & Steinmetz 1997; Sommer-Larsen, Gelato, Vedel, 1999; Navarro & Steinmetz 2000). In addition, N-body simulations' specific angular momentum distribution disagree with observations (mismatch of the specific angular momentum profile).

The over-cooling problem in CDM models (e.g., White & Reese, 1978; White & Frenk 1991) has often been considered responsible of the AMC: gas contracts into small clumps that collapse towards the center of the system, loosing angular momentum by dynamical friction, transferred to the DM halo (Navarro & Steinmetz 2000), when feedback effects heating the gas (UV background reionization, ram pressure, tidal heating) remain negligible. The problem reduces when some form of feedback is taken into account: e.g. energy feedback from supernova (Sommer-Larsen, Gelato, Vedel, 1999). However, other problems remain such as the mismatch of the angular momentum profiles (e.g., **van den Bosch, Burkert and Swaters, 2001, hereafter VBS**), or the logarithmic scatter of the spin parameter, smaller for real galaxies than in simulations (de Jong & Lacey 2000).

Gas processes can result in different distributions between DM and gas (Maller & Dekel 2002). In such model, low specific angular momentum baryons are eliminated by SF, that removes gas from small incoming haloes, since low angular momentum components of the system are provided by these small haloes (see also Sommer-Larsen et al. 2003; Abadi et al. 2004).

Indeed, unless a process like a "selective outflows" of low angular momentum gas (D'Onghia & Burkert 2004) is present, the combination of DF with feedback models, even in the absence of substructures, was long unsuccessful in forming bulgeless galaxies (van den Bosch et al, 2002). Nevertheless, bulge-less galaxies, with flat galaxy density profiles and angular momentum distribution of baryons resembling galaxies stellar disc recently resulted from stripping low angular momentum gas through supernovae explosions outflows (Governato et al. 2010).

In the present paper, we follow the path opened by Z12 and B13, but we consider another mechanism than SF that is also **better** able to flatten the density profiles of satellites. Namely, we use a mechanism based on the exchange of energy and angular momentum from baryons clumps to DM through dynamical friction (DF) (El-Zant et al. 2001, 2004; Ma & Boylan-Kolchin 2004; Nipoti et al. 2004; Romano-Diaz et al. 2008, 2009; DP09; Cole et al. 2011; Inoue & Saitoh 2011). We use **DP09** to calculate the flattening of isolated satellites through the mechanism based on DF, and a combination of the Taylor & Babul (2001) (TB01) model with **that** in P10 (hereafter TBP model) to study the effect of tidal stripping and heating on the satellites. In addition to the difference in the **cuspy to cored profile mechanism**, already present in B13, our model is properly taking into account**, through the TBP model, the tidal heating mechanism. Such tidal heating is not captured in the SPH simulations from which Z12 derive their correction (as stressed in Sect. 4 of B13), since, as they point out,** this would require a very high resolution (Choi et al. 2009). Moreover, we properly take into account disk shocking **while this is neglected in Z12: we account for the effects of satellites passing through the host galaxy disc**.

Finally, the Δv_c**-**$v_{\rm infall}$ **correction that we find shows a clearer trend (see the discussion in the following section)**. This is due to **the absence, in our case, of numerical effects present, and described, in Z12**[5] are not present.

In summary, although in our model the profile flattening is calculated as in Del Popolo *et al.* **(2014), here the model of Taylor & Babul (2001) is included to follow the dynamics of satellites and their interactions with the main halo, and to take into account the mass loss during substructure evolution due to tides and tidal heating. Moreover, inasmuch as inspired by Z12 and B13 in substructure treatment, we escaped the limitations of their SPH and SPH-based treatment with semi-analytic methods, obtaining a better** $v_c - v_{infall}$ **relation and accessing the effects of tidal heating and disc shocking. Our model employs a novel combination of parent-satellite interaction through dynamical friction, UV heating and tidal stripping to obtain satellite numbers and angular spin parameter distributions in agreement with observations.**

The paper is organized as follows. In Sect. 2, we describe how the CCP,**MSP and TBTF problem can be solved simultaneously when baryonic physics is properly taken into account, focussing more particularly on the latter two. Appendices A**

[5]The fact that gas-rich satellites in Z12 are **too rich is probably** due to inefficient stripping in their SPH simulations.

and B give the detail of the model. Sect. 3 describes the results, including in addition the solution to the AMC, and a discussion. Sect. 4 is devoted to conclusions.

2 Solving the small scale problems of ΛCDM

As previously reported, several solutions have been proposed to the MSP and TBTF problems (Strigari et al. 2007; Simon & Geha 2007; Madau et al. 2008; Zolotov et al. 2012; Brooks & Zolotov 2012; Purcell & Zentner 2012; Vera-Ciro et al. 2012; Di Cintio et al. (2012); Wang et al. 2012). B13 proposed an interesting baryonic solution to **those two problems: instead of running SPH simulations of different galaxies, they tried to introduce baryonic effects** in large N-body dissipationless simulations, like the VL2, showing that the result obtained is in agreement with observations of MW and M31 satellites.

In the following, we will partly follow their steps to obtain the corrected circular velocities and distribution of VL2 satellites. The differences between our model and Z12, and B13 has been reported in the introduction.

In summary the method is based on the following ideas and is divided into two main phases:

1. In the first phase, the satellite is considered isolated, **without interactions with the host halo, and the flattening of the density profile produced by baryonic physics is calculated (in particular, the lowering of the central mass of subhaloes). In this paper we deliberately chose not to take account of SF and to concentrate on the model of baryonic clumps exchanging energy and angular momentum with DM through DF, since it has clearly been shown (Del Popolo, 2014a, Fig. 4 reproduced here in Fig. 1) that in the mass (circular velocity) range of the dwarfs studied in the present paper, the former is less efficient in transforming cusps into cores than the latter. Del Popolo & Hiotelis (2014) compared also the result of the current model, adding SF, to the SPH simulations of Inoue & Saitoh (2012): the full model agrees with the results of Inoue & Saitoh (2012). The addition of SF does not alter the outcome significantly.**

2. Then comes the second phase, when the satellite**, no longer considered isolated, is now subject to the tidal field of the host halo, and finally accreted to it. The total central mass is further reduced, with respect to the first phase, by tidal stripping and heating. This latter decrease in the central mass can be expressed in terms of changes in the circular velocity, v_c, also proportional to the density. More precisely, we calculate the difference in circular velocity, at 1 kpc, between the DM-only (hereafter DMO) satellites** and those containing also baryons (hereafter DMB satellites), $\Delta v_{\rm c,1kpc} = v_{\rm c,DMO} - v_{\rm c,DMB}$.

   Then, the effects of baryon physics, not taken into account in N-body simulations, responsible of the flattening of the profile are introduced in the VL2 simulation by correcting the central circular velocity of the satellites.

In other words, **we obtain an analytical correction, similarly to Z12, to apply to the center of the haloes and that mimics the effect of flattening of the cusp, using tidal**

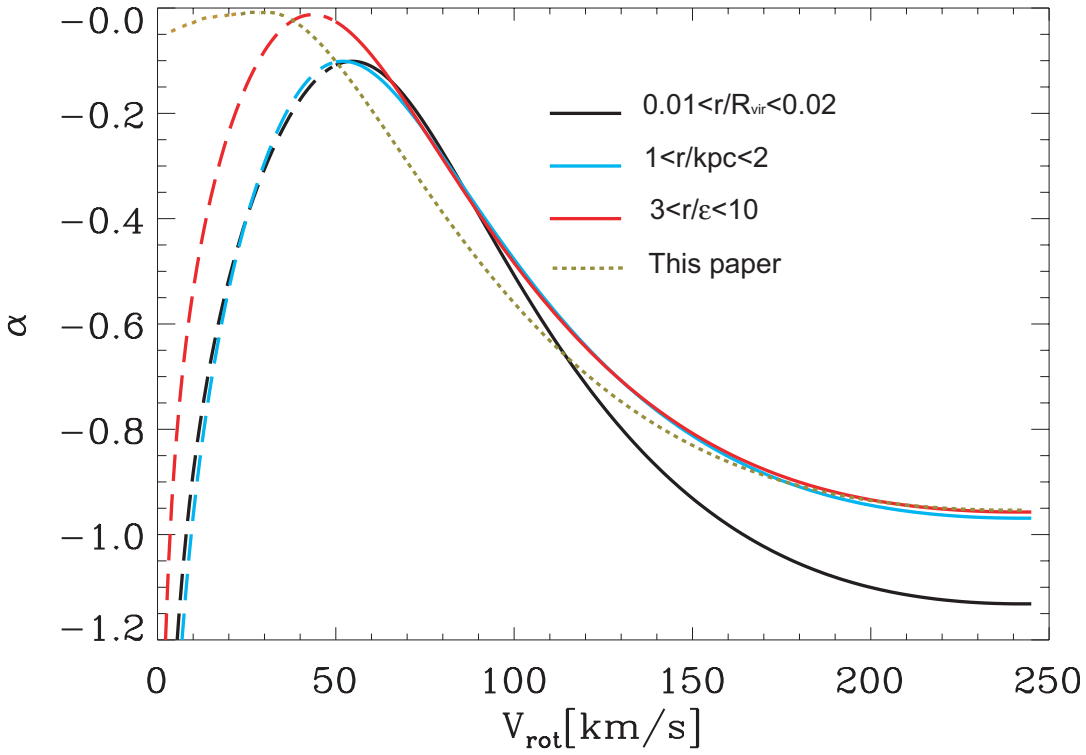

Figure 1. Logarithmic central density profile slope α vs. central circular velocity v_c from Del Popolo (2014a). The three plain lines correspond to three radial ranges for the result of Di Cintio et al. (2014), while the dotted line is our result. Extrapolations of the baryonic TF relation (Dutton et al. 2010) for stellar mass smaller than $10^9 M_\odot$ produce the dashed lines in the left side of their maxima. The Di Cintio results are based on the SF model, while ours uses the DF on clumps.

stripping and tidal heating (note that the latter effect is not taken into account in the Z12, as already reported above). To this we also join other corrections (e.g., tidal destruction and UV heating effects on subhaloes) discussed in DP09. Those corrections are then applied to the satellites of the VL2 simulation, as done by B13.

We stress again that in our model: a) the density profile flattening is due to DF and not to SF, as was the case in Z12 and B13; b) tidal heating, and disc shocking is taken into account, differently from Z12 and B13; c) our model does not suffer from the numerical effect **that was producing "artificially" rich satellites in Z12 simulations.**

2.1 First phase: density profile flattening and CCP

We first turn to the treatment of the isolated satellites, before **their** accretion onto the main system. The tidal forces of the parent halo on its satellite is fundamentally determined by the shape of the latter (e.g., Mashchenko et al 2006, 2008; P10). The structure of satellites with cuspy profiles does not suffer big changes while entering their parent halo, whereas cored profile satellites' gas will get easily stripped by the parent's tidal field, which, in some cases, even destroy that satellite (TB01; Stoher et al. 2002; Hayashi et al. 2003; Read et al. 2006; P10). **The first phase is thus of fundamental importance since it defines the shape of the satellite. Furthermore, it can equally be applied to study the parent or the**

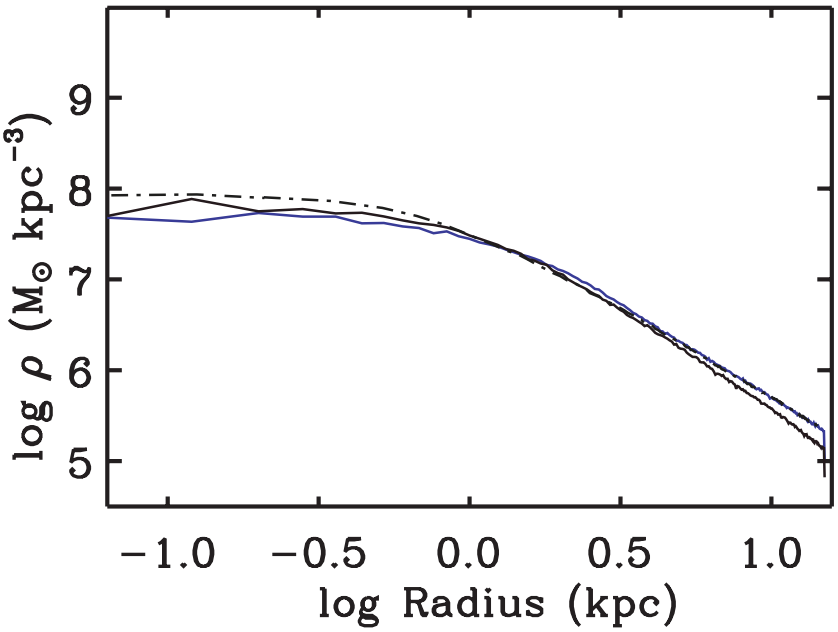

Figure 2. Reproduction of Fig. 3 from DP12b. Comparison of the DP12b dark matter density profile (dot-dashed line) with Governato et al. (2010) SPH simulations: galaxy DG1 (solid blue line) and galaxy DG2 (solid black line). Each model uses $v_{rot} \simeq 50 km/s$ and yields similar flattening from different methods.

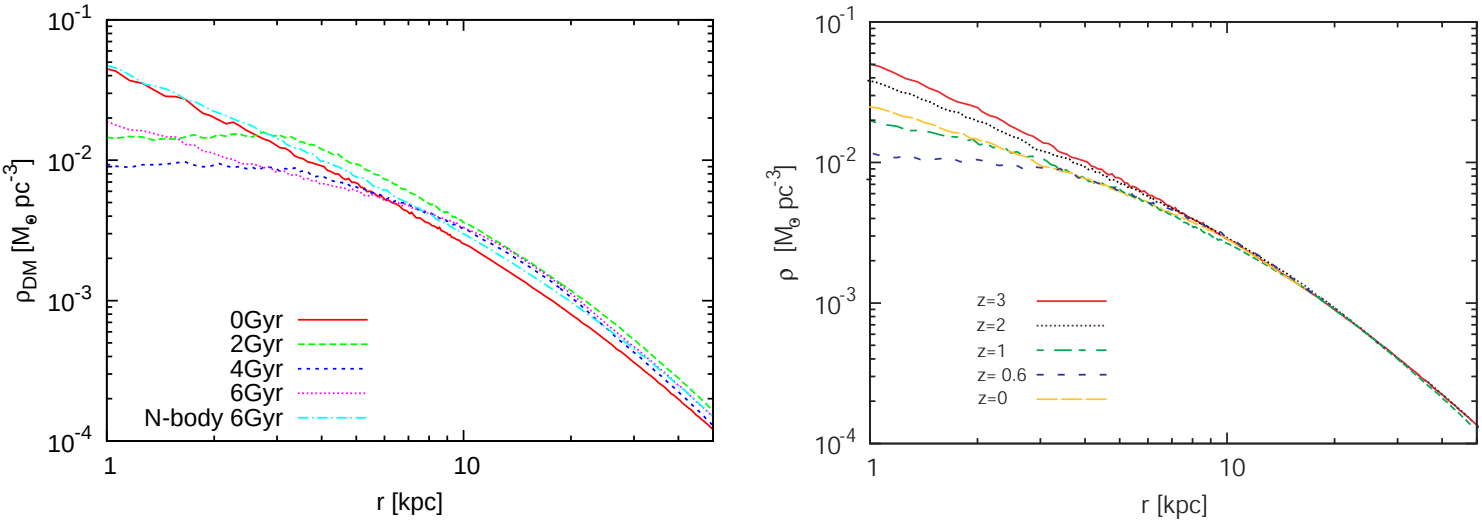

Figure 3. Reproduction of the density profile flattenings from Fig. 2 of Inoue & Saitoh (2011), left panel, and Fig.2a of Del Popolo & Hiotelis (2014), right panel. This compares the effects of baryonic clumps with SPH simulations and our model, respectively.

satellites density profiles flattening. We delve into it by applying Del Popolo (2009)'s model (DP09), summarized in Appendix A. **Such a model has been compared and tested against Governato et al. (2010) simulation-based model, in DP12b (Fig. 3, reproduced in Fig. 2, showing good agreement), and against SPH simulations**

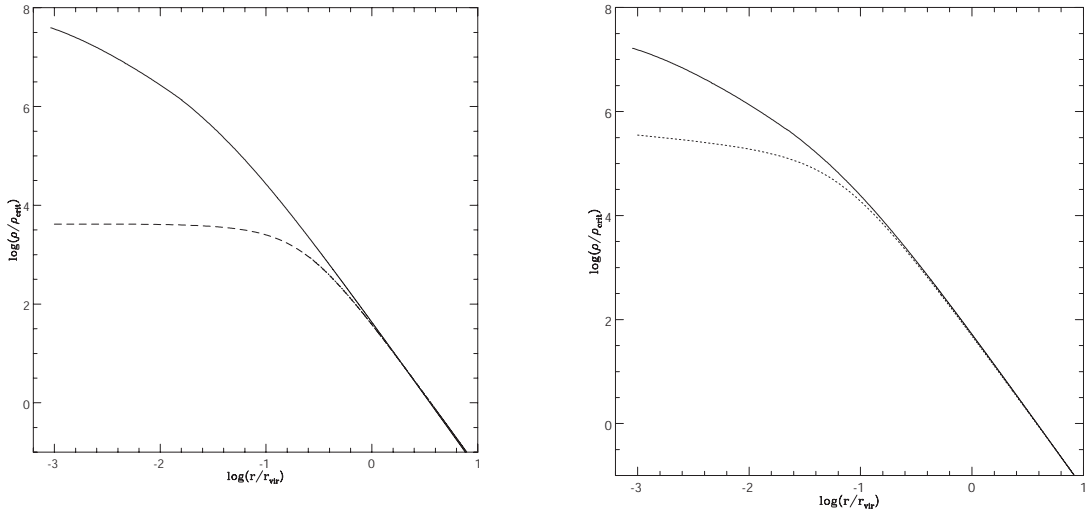

Figure 4. DM haloes profiles generated with the model of DP09 (see Appendix A). The solid line represents the DMO density profile**, while the dotted line,** the density profile with the effect of baryons, for respective masses and baryon fraction $10^8 M_\odot$ (panel a), $f_d = 0.004$ ($M_* \simeq 10^6 M_\odot$), and $10^{10} M_\odot$ (panel b), $f_d = 0.05$ ($M_* \simeq 10^8 M_\odot$). This offers a solution to the CCP.

of Inoue and Saitoh 2011, in Del Popolo and Hiotelis (2014, Fig. 2(a); we show both results from Inoue & Saitoh (2011) and Del Popolo & Hiotelis (2014) in our Fig. 3 for comparison). Note, in Fig. 2, that even if different methods were used, keeping $v_{rot} \simeq 50 km/s$**, the flattening due to the two mechanisms is similar.** We now set out the procedure.

As was done in DP09 (**and** also in DP12a, DP12b), we study the evolution of proto-structures from the linear phase until they form structures with galactic mass, and then **calculate** their density profiles. The model discussed in DP09 (**and** DP12a, b), is an improved spherical infall model (SIM) already discussed by **many** authors (Gunn & Gott 1972; Fillmore & Goldreich 1984; Bertschinger 1985; Hoffman & Shaham 1985; Ryden & Gunn 1987; Henriksen & Widrow 1995, 1997, 1999; Henriksen & Le Delliou 2002; Le Delliou & Henriksen 2003; Le Delliou 2008; Ascasibar, Yepes & Gottlöber 2004; Williams, Babul & Dalcanton 2004; Le Delliou, Henriksen & MacMillan 2010, 2011a, 2011b)[6].

Differently from previous SIMs, adiabatic contraction, dynamical friction (DF), random angular momentum, ordered angular momentum, gas cooling, and star formation (see the Appendix) are all simultaneously taken into account.

In **our model, galaxy** formation starts with the proto-structure, made of DM and gas, in its linear phase. The baryonic fraction is fixed following McGaugh et al. (2010). More precisely, we use the detected baryonic fraction, $f_d = (M_b/M_{500})/f_b = F_b/f_b$, which is the ratio of the actual baryon fraction, $F_b = M_b/M_{500}$, in the structure, to the amount of baryons expected from the cosmic baryon fraction, $f_b = 0.17 \pm 0.01$ (Komatsu et al. 2009). During infall, baryons compress the DM (adiabatic contraction (AC))**. They** are then subject to radiative processes, giving rise to clumps which condense into stars as described in Li et al. (2010) (Sect. 2.2.2, 2.2.3), De Lucia & Helmi (2008). Infalling baryon clumps suffer DF from DM particles, transferring energy and angular momentum to DM, which thus moves

[6]Changes to the spherical collapse introduced by dark energy where studied in Del Popolo, Pace, &Lima 2013; Del Popolo, Pace, & Lima 2013a, b.; Del Popolo et al. 2013.

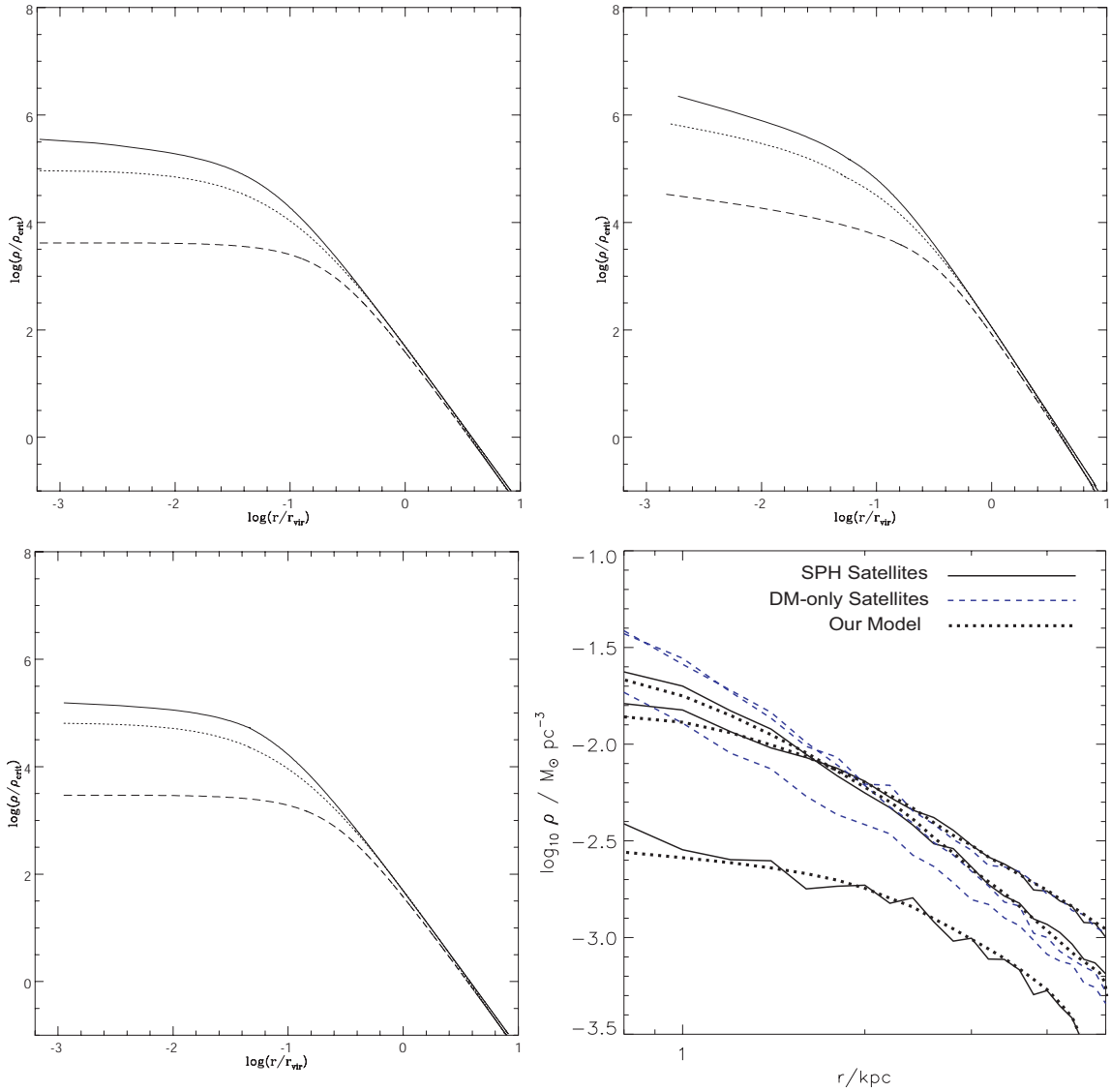

Figure 5. Changes of the density profiles **with baryonic fraction**. In Fig. 5a-c, the dashed line represents the density profiles with mass $10^8 M_\odot$, the dotted line those with $10^9 M_\odot$, and the solid lines those with mass $10^{10} M_\odot$. In Fig. 5a the baryonic fractions, f_d, are the same as in Fig. 4a, b, namely $f_d = 0.004$ for the halo of $10^8 M_\odot$, $f_d = 0.05$ for the halo of $10^{10} M_\odot$. In the case of the halo of $10^9 M_\odot$,we take $f_d = 0.04$. In Fig. 5b the baryonic fractions are reduced to $f_d/7$, and in Fig. 5c they are increased to $2f_d$. In Fig. 5d, we compare our model with Z12 results. Dark matter (DM) profiles of the three most luminous SPH satellites (solid lines), and DM-only counterparts (dashed lines) in Z12 are shown. The dotted lines are the results of our model relative to the SPH satellites.

towards the external parts of the structure and **hence** gives rise to the observed density profile flattening.

In Fig. 4, we plot the DM halo profiles generated with the model **from** DP09 (Appendix A). In the **left (resp. right**) panel, the solid line represents the density profile of **pure DM haloes with** $10^8 M_\odot$ **(resp.** $10^{10} M_\odot$**), while the dotted line gives the density profile in the case baryons are taken into account, in the left (resp. right) panel, with** $f_d = 0.004$ **(resp.** $f_d = 0.04$**), corresponding to a stellar mass of** $\simeq 10^6 M_\odot$ **(resp.**

$\simeq 10^7 M_\odot$) **(McGaugh et al. 2010),** with the model of DP09 (Appendix A).

As Fig. 4 shows, the density profile obtained from DM only (DMO) profile, is much steeper **in the centre** than the profile containing also baryons (DMB profile). They equally describe **on parents or satellite haloes the effects of baryons and such** flattening can solve the CCP. In Fig. 5a-c, we show the density profiles of satellites with masses equal to $10^8 M_\odot$ (dashed line), $10^9 M_\odot$ (dotted line), and $10^{10} M_\odot$ (solid line), respectively. The baryonic **fractions in Fig. 5a are similar to** Fig. 4a-b, namely $f_d = 0.004$ for the halo of $10^8 M_\odot$, $f_d = 0.05$ for the halo of $10^{10} M_\odot$, ascribing $f_d = 0.04$ for the halo of $10^9 M_\odot$ ($M_* \simeq 10^7 M_\odot$). In Fig. 5b, c, the baryonic fractions are **respectively reduced to** $fd/7$**, increased to** $2f_d$. Haloes having smaller baryonic fraction have steeper profiles (Fig. 5b), while larger content of baryons flattens further the profile (Fig. 5c). In Fig. 5d, we compared our results with the most luminous and gas rich satellites of Z12 (see their Fig. 2). In our plot the dashed lines **represent** the Z12 DMO satellites, the solid lines **give** the Z12 DMB satellites, while the dashed lines represent the result from our model for the DMB satellites. The plot shows the flattening of the density profiles with respect to the DMO satellites when baryons are taken into account, **as well as** a good agreement between our model and the Z12 result.

As shown in Table 2 of Boylan-Kolchin, Bullock, & Kaplinghat (2012), the **bright MW dSPhs with smallest** $V_{\rm max}$ **is Carina, with** $V_{\rm max} = 11.4^{+1.1}_{-1.0}$ **and mass** $1.8^{+1.8}_{-0.9} \times 10^8 M_\odot$**, while that with largest** $V_{\rm max}$ **is Draco with** $V_{\rm max} = 20.5^{+4.8}_{-3.9}$ **and mass** $1.2^{+2.0}_{-0.7} \times 10^9 M_\odot$. Their M_V magnitude is in the range $M_V \simeq [-8, -14]$.

We generate haloes with circular velocity in the range $V_c = 10 - 50$ km/s. Following Klypin, Trujillo-Gomez, and Primack (2011), the circular velocity, $v_{\rm c}$, of subhaloes can be converted into the subhalo mass by means of

$$V_{\rm c} = 3.8 \times 10^{-2} M^{0.305} \tag{2.1}$$

Given a halo mass, we calculate its DMO density profile, ρ_{DMO}, and its DMB density profile, ρ_{DMB}. We then may calculate the circular velocity at 1 kpc, $v_{\rm c,1kpc}$, for the DMO density profile recalling that

$$\rho(R) = \frac{1}{4\pi G}\left[2\frac{V}{R}\frac{\partial V}{\partial R} + (\frac{V}{R})^2\right] \tag{2.2}$$

(de Blok et al. 2001; Governato et al. 2012). Similarly, we calculate the $v_{\rm c,1kpc}$ for the DMB satellites, and finally $\Delta v_{\rm c,1kpc} = v_{\rm c,DMO} - v_{\rm c,DMB}$. Obviously, if we calculate $\Delta v_{\rm c,1kpc}$ at this stage, we would not take into account the further reduction of the satellite mass due to its interaction with the parent halo, because of tidal stripping, and tidal heating. **The next subsection studies this side of the problem.**

2.2 Second phase: mass lost caused by tidal stripping and tidal heating

Here starts the second phase previously mentioned, that considers the effects of the interaction between the main halo and the satellite.

In order to **properly take into account tidal stripping and heating after infall, and to get accurate** v_{max} **values, we follow a combination of TB01 model with** P10 models. The model is described in Appendix B. **In TB01, the model is compared with high resolution simulations, while P10 checks their model in its Appendix A through high resolution N-body simulations.**

The TB01 model is able to follow the merger history**, growth of the interacting satellites and to track the substructure evolution, taking into account the mass**

loss due to tidal stripping, tidal heating, as well as enhancement of stripping due to the disc, in the host halo. P10 studied the effect of the shape **of satellites (cusp, core), and of the presence of a baryonic disc on satellite populations around spiral galaxies.** He also constructed a semi-analytic model describing the satellites tidal evolution **during their fall into the host galaxy** that displayed good agreement with his simulations. The P10 model is fundamentally based on TB01, with the difference that **the TB01 model is more complete** since it also takes into account tidal heating. **In our model we use the DM density profile for the host halo chosen by P10, namely a NFW profile, but** with the parameters from P10. **Nonetheless, similarly to P10 and contrary to TB01, we did not take into account the bulge.**

This was neglected (as in P10) since the disc has a much larger mass than the bulge, and the density gradient of the disk is 10 times larger than that of the bulge or of the halo, thus heating the satellites 100 times more efficiently than the other components.

The semi-analytic model, **hereafter indicated as TBP model, is described in Appendix B.**

At this point we may put together the mass decrease in satellites due to phase 1 (core flattening due to interaction of baryonic clumps with DM), and **due to tidal stripping and heating.**

In Fig. 6 we plot the difference in circular velocity at 1 kpc, and at $z = 0$, for the DMO and DMB satellites. The changes in velocity, $\Delta v_{\rm c,1kpc} = v_{\rm c,DMO} - v_{\rm c,DMB}$, are due to the cumulative effects of the two phases previously discussed, namely a) the cuspy to cored transformation of density profiles due to the interaction **between** baryon clumps and DM through dynamical friction, and b) tidal stripping and heating produced by the passage of the satellite **through** the host galaxy. The dashed line is a fit to the data, and is given by

$$\begin{aligned} \Delta(v_{1kpc}) &= 0.3{\rm v_{infall}} - 0.3{\rm km/s} \\ & 10{\rm km/s} < {\rm v_{infall}} < 50{\rm km/s} \end{aligned} \tag{2.3}$$

We want to stress again that **this correction is then** applied to VL2, together with the other corrections discussed in what follows.

The correction **obtained is close to the results from Z12 that accounted for the reduction of subhaloes central mass produced by SF and tidal stripping,** given by

$$\begin{aligned} \Delta(v_{1kpc}) &= 0.2{\rm v_{infall}} - 0.26{\rm km/s} \\ & 20{\rm km/s} < {\rm v_{infall}} < 50{\rm km/s} \end{aligned} \tag{2.4}$$

The above equation, from Z12, was obtained by fitting the **corrected data displayed on** their Fig. 8. Our Fig. 6**, which displays our corrections to the same original data,** shows a **clearer trend Δv_c-$v_{\rm infall}$, due to the absence of the numerical effect described in Z12,** namely the fact that their gas-rich satellites are probably richer due to inefficient stripping in their SPH simulations **(recall Sect. 4 of B13, where such effects are discussed). We stress out that our model properly takes into account tidal heating through the TBP model while this is not taken into account in Z12. It also correctly account for the passing of satellite through host disk that induces disk shocking, while again, Z12 neglects it. The former lack is recognised, as discussed, in Z12 itself and in B13, where in addition the absence of disk shocking also pointed in Z12 as leading to slower satellite disruption. In fact, as discussed in B13, it can be recognised that the simulations of Z12 having**

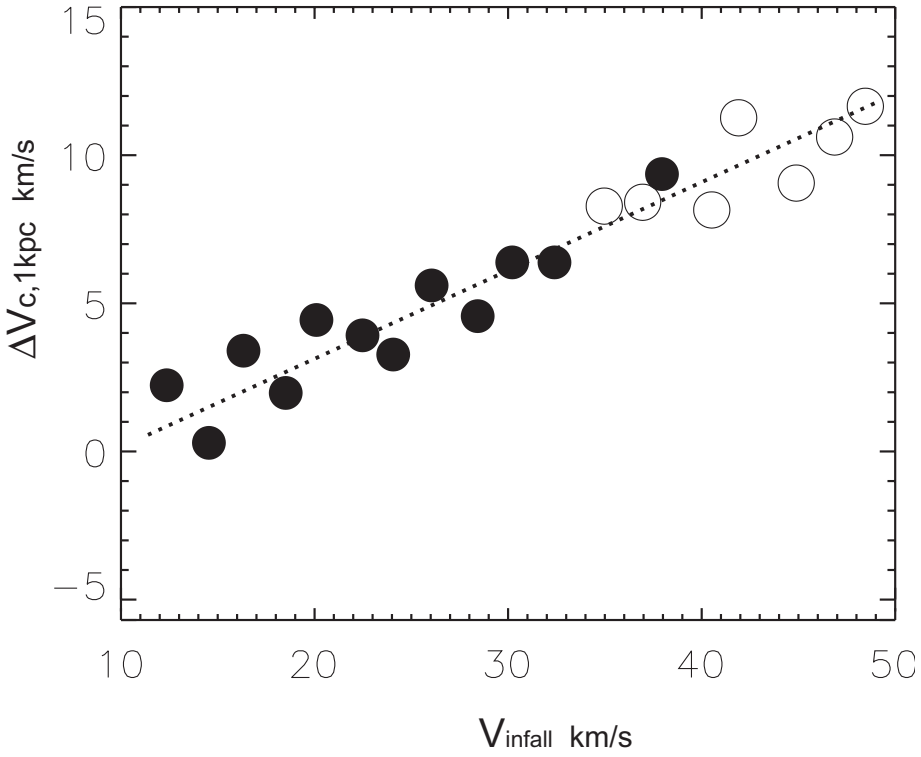

Figure 6. Difference in $v_{\rm c}$ at 1 kpc, and at $z = 0$, between DMO, and DMB satellites in terms of $v_{\rm max}$ of the DMO satellites at infall.

indeed disk shocked satellites, those are discarded as outliers by their scheme since their correction, neglecting disk shocking, lead to very strong disruptions and eccentricities compared to other subhalos.

Equation (2.3) gives the difference between DM and SPH runs, and therefore the corrections to apply to satellites in N-body simulations to take account of the missing piece of baryonic physics.

In the case of $v_{infall} = 30$km/s**, the Z12 correction gives** $\Delta(v_{1kpc}) = 5.74$**, while ours** gives $\Delta(v_{1kpc}) = 8.7$. The difference between the two $\Delta(v_{1kpc})$ is due to the different models used to produce the pre-infall flattening of the satellites density profile and the tidal heating of subhaloes (Gnedin et al. 1999; Mayer et al. 2001; D'Onghia et al. 2010b; Kazantzidis et al. 2011). Whereas the latter is taken into account by our model, it cannot be captured in the **Z12 correction, using SPH simulations, (as stressed in Sect. 4 of B13)** since this would have required a very high resolution (Choi et al. 2009).

Concerning the pre-infall flattening, the models are qualitatively distinct: in Z12 it is due to SF, and in our case is connected to DF. As shown by Cole et al. (2011), DF on infalling clumps is a very efficient mechanism in flattening the DM profile. A clump having a mass of 1% of the halo mass can give rise to a core from a cuspy profile removing twice its mass from the inner part of the halo. In the case of the SF the mechanism becomes less effective

when going to lower masses (e.g., dwarfs with stellar mass $< 10^5 - 10^7 M_\odot$ have fewer stars and supernovae explosions are as a consequence less present with respect to dwarfs having stellar mass $> 10^7 M_\odot$ (Governato et al. 2012)).

2.3 Evaluation of luminous satellites

We have thus seen that the number of massive satellites is reduced by applying baryonic corrections, taken into account by Z12 or in the present work, to dissipationless N-body simulations, and in particular to the satellites in VL2. We are then left with the task to determine whether indeed the baryonic corrections also reduce the number of luminous satellites, and if this number is in agreement with those observed in the MW. In order to check this, other corrections are needed.

Our correction (Eq. 2.3), similarly to the Z12 correction, applies to satellites that survived at $z = 0$, with their central v_c reduced by baryonic physics. **furthermore**, other satellites are destroyed (by e.g. stripping or photo-heating) before $z = 0$. In N-body simulations, like the VL2, **baryonic** effects are not taken into account. **Some satellites of such simulations will not be destroyed when the same satellites may be totally destroyed by enhanced tidal stripping (due to the presence of a disc) in the real universe or even SPH. Our method requires then to determine** the destroyed satellites before applying our Z12-like correction to VL2. To evaluate the luminous satellite population, we require two additional corrections: a) to account for the destruction by tidal stripping, b) and to account for suppression in star formation.

The first correction to apply to **VL2 N-body satellites is the destruction rates by tidal stripping. To do so,** we need a relation between the mass retained since the infall and the change in the velocity (e.g., $v_{\rm max}$) in the same time interval.

We computed that relation using the **same** satellites with which we calculated the relation $\Delta v_{\rm c,1kpc}$-$v_{\rm infall}$ (see the final part of sect. 2.1).

We plotted the result in Fig. 7. The filled circles represent the DMB satellites having baryonic fraction $M_b/M_{500} > 0.01$, while the open circles show the DMB satellites with baryonic fraction $M_b/M_{500} < 0.01$. The open diamonds represent the DMO satellites.

The plot shows that DMB satellites loose more mass than **DMOs**. This difference is due to the following reasons: 1) DMB satellites contain gas, contrary to **DMOs**; 2) DMB satellites have flatter profiles than **DMOs and thus** suffer more tidal stripping (e.g., P10). The same goes between the baryon-richer DMB (filled circles) and baryon-poorer DMB (open circles). The maximum loss happen for DMB satellites in the vicinity of the host galaxy disc.

In Fig. 7, we also plotted the analytic results from Eq. 8 of P10 (see also their Fig. 6), describing the change in $v_{\rm max}$ as a function of mass lost due to tidal stripping

$$\frac{v_{\rm max}(z=0)}{v_{\rm infall}} = \frac{2^\zeta x^\eta}{(1+x)^\zeta} \tag{2.5}$$

where $x \equiv mass(z=0)/mass(z=infall)$.

The dashed line represents the previous equation for central density profile logarithmic slopes $\gamma = 1.5$**, yielding** $\zeta = 0.40$ **and** $\eta = 0.24$**, the solid line stands for the case**

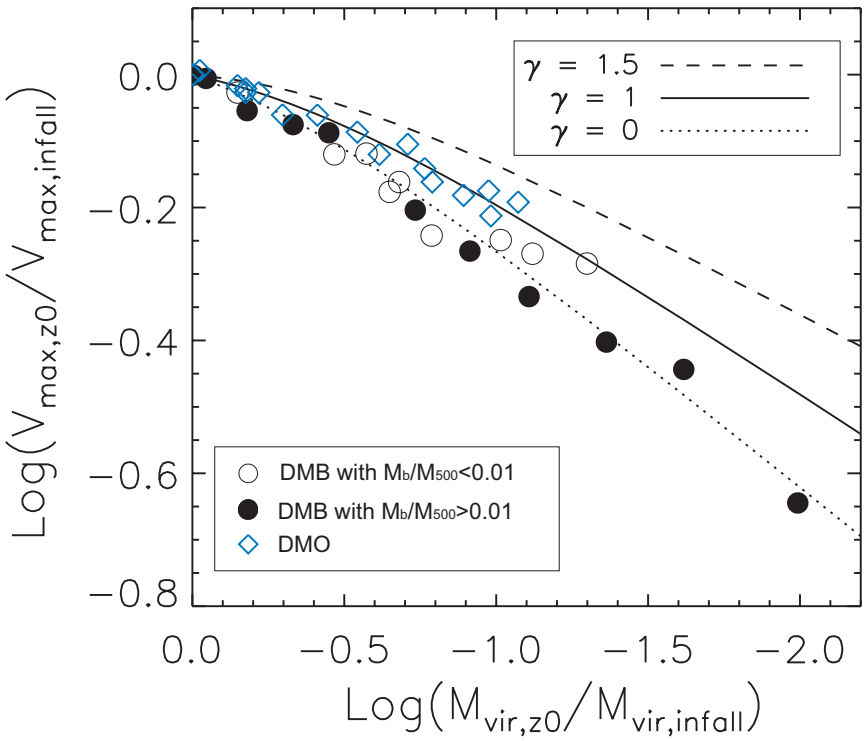

Figure 7. Change in the circular velocity at 1kpc between $z_{\rm infall}$ and $z = 0$ in terms of the retained mass. Filled circles represent the DMB satellites having baryonic fraction $M_b/M_{500} > 0.01$, while open circles, the DMB satellites with baryonic fraction $M_b/M_{500} < 0.01$. The open diamonds represent the DMO satellites. The dashed, solid, and dotted lines represents Eq. 8 of P10 for slope $\gamma = 1.5, 1, 0$, respectively.

$\gamma = 1$**, for which** $\zeta = 0.40$ **and** $\eta = 0.30$**, and the dotted line covers the case** $\gamma = 0$**, with** $\zeta = 0.40$ and $\eta = 0.37$, respectively.

The $\gamma = 1$ **curve in Fig. 7 gives a good fit to the change in** $v_{\rm max}$ **for the DMO satellites, which generally produce cuspy density profiles.** Conversely, the $\gamma = 0$ curve presents a good approximation for the DMB satellites, that generally should be cored, particularly for those having large baryonic content (i.e., many stars).

Summarizing, we may determine which VL2 satellites are **tidally disrupted by fixing a destruction criterion** (e.g., mass lost), and by using Eq. (2.5). Since the VL2 satellites are obtained in N-body only simulations**, their inner slopes is expected to be** $\gamma \simeq 1$**, as found in B13. Consequently, we must use** $\zeta = 0.40$ **and** $\eta = 0.30$ **in Eq. (2.5).**

As for the destruction criteria, we fix it similarly to B13, as follows.

As already discussed, tides affect much more cored than cuspy satellites. **Under these conditions, the latter may survive, loosing up to 99.99% of their mass, while the former** are disrupted. In the case of cored satellites, for which $\gamma = 0$, and a host galaxy with $\gamma = 1$**, Fig. 2 in P10 shows that those satellites with pericenters** $\lesssim$ **20 kpc loose, when the host galaxy has a disc,** 99.9% of their mass, and 90% if there is no disc. Here we assume, as B13, that **VL2 satellites are disrupted if they loose** $> 90\%$ **of their**

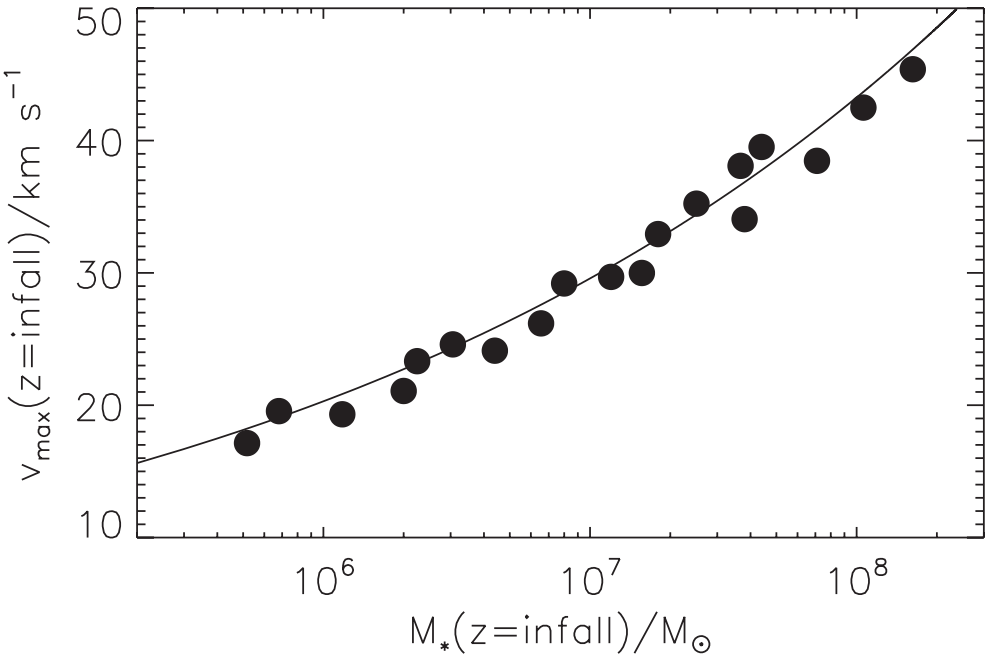

Figure 8. Values of $v_{\rm max}$ of the DMO subhaloes as function of the stellar mass, M_*, at infall. The solid line, the fit to the data **given by** $\frac{M_*}{M_\odot} = 0.1(\frac{v_{\rm infall}}{\rm kms^{-1}})^{5.5}$, indicates how stellar mass change with $v_{\rm infall}$.

mass after infall and pass at a distance < 20 kpc from the host galaxy center. **As these criteria are valid for cored satellites, we should therefore select a criterion to establish** whether a satellite is cored or cuspy. Governato et al. (2012) found that satellites having a stellar mass $> 10^7 M_\odot$, corresponding to $v_{\rm infall} > 30$ km/s, are cored. We recall that, in their simulation, the flattening is produced by SF, while in our model**, it** is connected to DF. In the following, as in B13, we apply the disruption criteria discussed above to satellites with $v_{\rm infall} > 30$ km/s. In the case $v_{\rm infall} < 30$ km/s, the halo is fully stripped off only if it loose 97% of its mass (Wetzel & White 2010).

Summarizing**, all the VL2 satellites loosing more than 97% mass** ($x = 0.03$)**, or loosing more than 90% mass, combined with** $v_{\rm infall} > 30$ **km/s and a pericentric passages** $< 20kpc$**,** are considered to be destroyed.

The second correction is the suppression of star formation by photo-heating, obtained from the Okamoto et al. (2008) results. In their paper, **a uniform ionizing background is assumed**, for which He II reionization happens at $z = 3.5$, while **it occurs at** $z = 9$ **for H and He I.** They found the value of the typical halo mass **retaining** 50% of f_b: $M_t(z)$. This mass can be converted into a typical velocity, $v_t(z)$[7]. Thus, if a VL2 subhalo has a larger peak velocity**,** $v_{\rm peak} > v_t$[8]**, it is considered to contain** enough baryons to make it luminous.

[7] In the conversion, we used an overdensity $200\rho_{\rm crit}$, and a WMAP3 cosmology (Spergel et al. 2007).
[8] $v_{\rm peak}$ represents the largest value of $v_{\rm max}$ over the entire history of the subhalo.

The last step consists in assigning a luminosity to the surviving satellites. **We first need to allocate stellar masses to VL2 satellites via a relation between $v_{\rm infall}$ and the stellar mass M_*.**

To do so, we recycled the satellites considered in the determination of $\Delta v_{\rm c,1kpc}$. **As it is usually assumed (Bullock et al. 2000; Kravtsov et al. 2004; Strigari et al. 2007; Bovill & Ricotti 2011; Simha et al. 2012),** we associated the DM-only subhaloes with their most massive satellites, at formation or accretion time.

Fig. 8 plots $v_{\rm infall}$ in terms of the stellar mass, M_*. The $v_{\rm infall}$-M_* relation is obtained by fitting the data, **yielding** the relation[9]

$$\frac{M_*}{M_\odot} = 0.1(\frac{v_{\rm infall}}{\rm kms^{-1}})^{5.5}. \tag{2.6}$$

Finally, we need to relate M_* and the V-band magnitude, $M_{\rm V}$. We apply the relation from B13, extracted from Z12 simulations,

$$\log_{10}(\frac{M_*}{M_\odot}) = 2.37 - 0.38 M_{\rm V}. \tag{2.7}$$

3 Results and discussion

The result of the **corrections discussed above are plotted in Fig. 9. The top panel represents** the results from VL2 at $z = 0$. The bottom panel **presents the results of applying those corrections (heating, destruction, and velocity corrections) on the same satellites. The objects considered "observable" in the VL2 simulation are ascribed red filled symbols**. Dark objects are marked by empty circles: **simple empty circles have a mass smaller than the minimum to retain baryon and form stars, while objects crossed in addition with an "x", represent subhaloes that do not survive to the baryonic effects (e.g., baryonic disc, etc).** Finally, filled black circles are satellites that lose 90% of their mass since infall, but do not satisfy the destruction criteria previously described: stripped of their stars, they actually appear much fainter than the "observable" ones.

Note that the Z12 correction was not applied to satellites with $v_{max} > 50$km/s**(for example, satellites with $M_V < -16$, as they are the 5 most massive satellites at infall).**

We obtain 3 satellites with $v_{1kpc} > 20$ km/s, in agreement with B13. However, our central velocities are smaller: the correction to the circular velocity, $\Delta(v_{1kpc})$, is larger in our model compared to Z12 and B13. In addition, in our case, some satellites are "overcorrected": their corrected velocities are negative.

Similar to B13, overcorrected haloes are part of a population that lost a great part of their mass after infall. At $z = 0$, their circular velocity at 1 kpc, v_{1kpc}, is very low so the correction $\Delta(v_{1kpc})$ brings them to negative values. After infall, that population suffers **mass loss larger than 99.9%** and exhibit tidal radii < 1 kpc. It can therefore be considered as a population of destroyed subhaloes.

It is interesting to note from Fig. 9 that the model obtains not only a reduction of the number of satellites, solving the MSP, but also a reduction of their central velocity, clearing up the TBTF problem.

[9]Note that tidal stripping and heating from $z_{\rm infall}$ to $z = 0$ **produce a reduction in the halo masses**, introducing scatter in the $v_{\rm infall}$-M_* relation at infall.

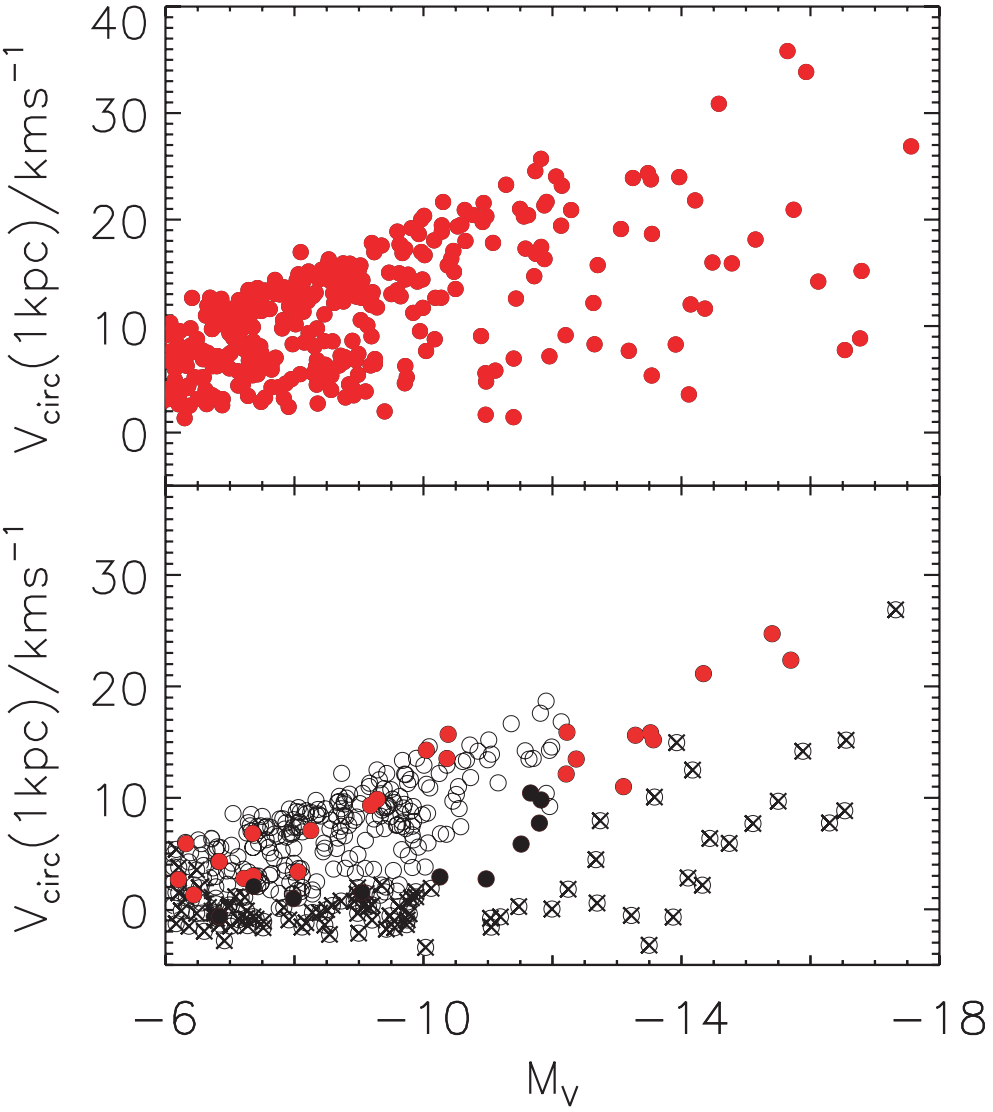

Figure 9. Plot of v_{1kpc} vs M_V for the VL2 simulation subhaloes. In the top panel, we plot the raw VL2 satellites velocities vs M_V at $z = 0$, as in B13. In the bottom panel, we **present them after the baryonic corrections described in the text.** The filled black circles represent satellites that have lost enough mass so that their stars are stripped and their luminosities are just upper limits, while their actual luminosities are much fainter at infall. Filled red circles are satellite actually observable at $z = 0$**. Dark subhaloes are represented by empty circles, while circles with an x are subhaloes that have low probability to survive to tidal effects.**

As for B13, UV heating and tidal destruction are necessary to reconcile the total number of luminous satellites with observations, while the Z12 correction is necessary to reconcile the masses of the subhaloes with observations.

If the baryonic effects **were not taken into account, a population would exist** of satellites significantly more massive than those of the MW.

Finally, the effect of UV heating is required, on top of tidal destruction, to get the correct number of luminous satellites.

A similar result has been obtained in a series of papers (Z12; Brooks & Zolotov 2012; B13). In those papers**and differently from our model, the main effect is connected to SF following episodic bursts of supernovae, that produce the flattening of the cusp and the TBTF solution.**

In our model, the solution to the aforementioned problems is connected to the complex interaction between DM and baryons mediated by DF. Our study is similar to those of El-Zant et al. (2001, 2004), Romano-Diaz et al. (2008), Cole et al. (2011), in the sense that DF plays an important role. However, **while previous studies considered one effect at a time (e.g., random angular momentum, angular momentum generated by tidal torques, adiabatic contraction, cooling, star formation), we consider the joint effect of all of them.**

Our model differs from Z12 and B13 not only, as already mentioned, on the fundamental mechanism producing the flattening of isolated haloes' density profile, but also on the model describing the satellites dynamics.

Indeed, here the dynamics of the satellites (i.e., the TBP model in Appendix B) **proceeds from** two competing mechanisms: dynamical friction, **inducing** a decay of the satellites orbits, and tidal stripping and heating, reducing the bound mass of the satellite. This reduction causes a decrease in the frictional force, which produces in turn a slowing down of the orbital collapse. Massive and dense satellite are more subject to DF and sink fast towards the center of the potential. Low-density satellites are more subject to stripping and fall slowly towards the center. Mass loss and tidal heating depend primarily on the satellite density profile, as confirmed by P10.

Here, tidal heating and disc shocking are taken into account through the TBP model, in contrast with B13 (as stressed in Sect. 4 of B13)[10]. In SPH simulations (Z12 simulations in our case) it is difficult to capture tidal heating, since this would require a very high resolution (Choi et al. 2009).

Accounting for these effects speeds up the disruption of satellite, and yields a further reduction of the mass retained by **them** compared with B13. As already reported, a **satellite disc-crossing** results in a 100 times more heating **than if** provoked by the halo component or by the bulge (**should this component be** considered) **of the parent.**

Tidal heating increases mass loss, reducing dynamical friction, with the final result of a slower sinking of the satellite. The more inclined an orbit is, the more heating is active. **Considering as** disrupted a satellite that has lost 90% of its mass, heating reduces the disruption time by 40%. Moreover, heating outputs a different distribution of stripped material in satellites. **Finally and as mentioned, because of the absence of the numerical effect found in Z12 that resulted in their inefficient stripping of gas-rich satellites in their SPH simulations, our Δv_c-$v_{\rm infall}$ correction displays a clearer trend.**

In the present paper, we partially realized the suggestion of B13 to adopt a semi-analytic model (two in our case) to follow the growth, and merger history, of satellites in order to single out those which retain gas to form stars. We even pushed a step further by incorporating in the semi-analytic model the effects of UV heating, and by applying directly the model to the VL2 satellites. **Our** models call for the generation of a large sample of satellites with similar properties to those displayed in the VL2 subhalo catalog (Diemand et al. 2008).

[10]B13 is based on Z12 results. In Z12, some haloes experienced disc shocking **and** were strongly disrupted**. For this, they** were considered outliers, and not used in the calculation in the Z12 correction.

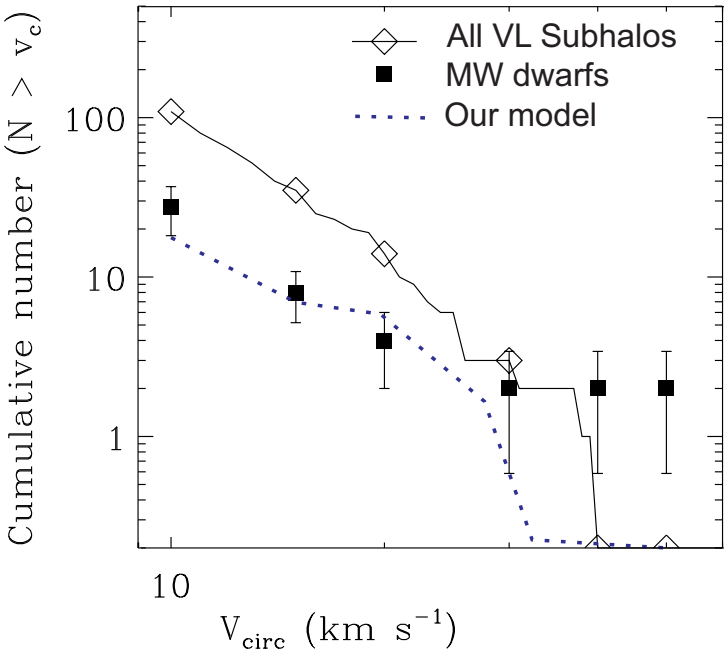

Figure 10. Cumulative number of MW satellites in terms of circular velocity. The filled squares display the classical MW plus ultra-faint-dwarfs in Simon & Geha (2007). The solid line with diamonds represents the abundance of the Via Lactea subhaloes (Diemand et al. 2007). The dashed line shows the abundance of subhaloes from VL2 after the baryonic corrections discussed in the text.

Then, applying the model in Appendix A, we may follow the formation of the satellites, and, by means of the model in Appendix B, we may study their dynamics, the mass loss due to tidal stripping, tidal heating, and the effect of the central baryonic disk. B13 emphasized the enhancement of tidal stripping that a disk would produce, but they used a correction (from Z12) that neglects disk shocking. To be more precise, Z12 considered the few satellites experiencing disk shocking to be outliers (see B13). In Z12, and then B13, tidal heating was not accounted for as it would have required very high resolution to be captured (Choi et al. 2009).

In Fig. 10, we compared the cumulative number of MW satellites in terms of the circular velocity of the halo with theoretical results. The upper solid line with diamonds represents the Via Lactea subhaloes (Diemand et al. 2007). The filled squares display the set of the sum of the classical MW dwarfs and the ultra-faint-dwarfs (Simon & Geha 2007). The dashed line shows the result of our model in terms of the abundance of subhaloes in the VL2 simulations after the baryonic corrections discussed. This plot demonstrates clearly how applying the baryonic correction to the VL2 subhaloes reduces the number of the satellites to reach the levels observed in the MW, thereby solving the MSP.

Since our model is not so computationally "heavy" as SPH simulations, we can study the MSP in different galaxies. To solve the problem in a single galaxy is not enough to conclude that the problem is solved in galaxies different from ours. In fact, several authors have discussed the MSP in relation to the host galaxy mass. Di Cintio et al. (2012), Vera-Ciro et al. (2012), Wang et al. (2012), showed that if the MW true virial mass is smaller than $10^{12} M_{\odot}$, namely $\simeq 8 \times 10^{11} M_{\odot}$, the satellites excess may disappear.

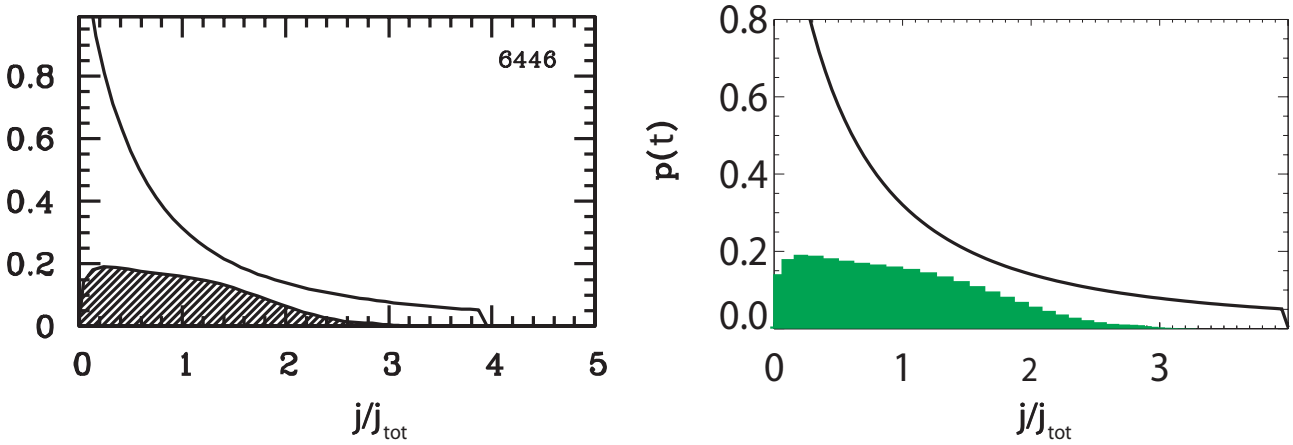

Figure 11. The AMD for UCG 6446, obtained by van den Bosch, Burkert, & Swaters (2001) (left panel, shaded area) compared to the AMD obtained with our model (right panel, filled area), and to the DM AMD from Bullock et al. (2000) (solid lines). The baryonic matter with highest and lowest momenta is absent from the disc.

In any case, the main point of our study, despite **it having room** for improvements, is that baryonic physics is able to solve simultaneously the MSP, and TBTF problem.

Several studies showed how tidal stripping and heating can solve the problem of satellites abundance, the MSP (e.g., Bullock et al. 2000; Kravtsov et al. 2004; Simon & Geha 2007; Peñarrubia et al. 2012), but their satellites' masses remained too high (TBTF problem). In our model, **we solve simultaneously both problems by taking into account the flattening of the density profiles of the satellites before infall, which renders them more sensitive to tides, the tidal stripping and heating resulting from infall and the enhancement of tide effects due to the baryonic disk.**

At the same time, our model solves the CCP, as shown in Sect. 2, through **DF energy and angular momentum transfer from baryon clumps to DM.** Finally and as shown in DP09 and Del Popolo et al. (**2014a**), the model also solves the "angular momentum catastrophe", that is the discrepancy in disk size and angular momentum distribution between the Smooth Particle Hydrodynamics (SPH) simulations of disk galaxy formation and real galaxies observations. In Fig. 11, we plot the angular momentum distribution (AMD) for UCG 6446 obtained by van den Bosch, Burkert, & Swaters (2001) (shaded area, left panel) compared to the AMD obtained with our model (filled area, right panel) and to the DM AMD obtained by Bullock et al. (2000) (solid lines). In the disc, the baryonic matter with lowest and highest momenta is absent. The angular momentum catastrophe is not present in our model because of the fact that the less massive clumps acquire more angular momentum than larger ones: in the virialization process smaller clumps loose more angular momentum than lager ones. As a result, the low tail in AMD is missing (see Del Popolo et al. **2014a** for a wider and deeper discussion).

Summarizing, the model shows how taking account of baryon physics allows to solve the small scale problems of the ΛCDM model.

4 Conclusions

In the present paper, we looked for a common solution to the CCP, AMC, MSP and the TBTF problem using two semi-analytic models: a) the model presented in DP09 (see also DP12a, b), and b) the model in TB01, and P10 (TBP model).

The study was divided into two phases: in the first**, satellites were considered isolated and we studied, by means of the DP09 model, how the haloes profile are changed by** adiabatic contraction, dynamical friction and the exchange of angular momentum, ordered and random, between baryons and DM**. This applies both to isolated satellites and parent haloes alike, and solves the CCP.**

The model had already shown in DP09, DP12a,b, that the angular momentum **generated through tidal torques and random velocities (random angular momentum) in the system, can be transferred in part to the DM from baryons through DF.** This produces a flattening of the cusp in agreement with previous studies based on DF (El-Zant et al. 2001, 2004; Romano-Diaz et al. 2008; Cole et al. 2011) and SF (Navarro et al. 1996a; Gelato & Sommer-Larsen 1999; Read & Gilmore 2005; Mashchenko et al. 2006, 2008).

In the second phase, **satellites were allowed to interact with the host halo, and tidal stripping and heating were** calculated through the TBP model.

We **obtained a correction to the central velocity of the satellites from the cusp to core transformation before the satellites are accreted, and tidal stripping and heating produced from interaction** with the main halo. This correction is close to that of Z12.

We then found the relation between the retained mass of satellites and the changes in $v_{\rm max}$ from $z_{\rm infall}$ to $z = 0$, and found a connection between mass loss and velocity change, in agreement with Eq. 8 of P10. This allowed us to determine the number of fully disrupted satellites because of tidal stripping and heating.

This correction, together with the effect of UV heating, and some criteria to fix which satellites are destroyed by tides, were applied to the VL2 satellites. As a result, the number of satellites is reduced and in agreement with the number observed in the MW. Similarly, the central velocity of satellites is reduced by the aforementioned corrections, supressing the angular momentum catastrophe.

The present paper shows that baryonic physics is of fundamental importance to solve the small scale problems of the ΛCDM model: the MSP, the TBTF problem, the CCP (DP09), and the AMC (DP09). The possibility to solve those problems in the ΛCDM paradigm without the need to change the power spectrum or the constituent particles of DM is another proof of the robustness of the ΛCDM paradigm, and should, in addition, spur further studies in the direction followed in the present paper.

Acknowledgements

A.D.P. would like to thank the International Institute of Physics in Natal for the facilities and hospitality, Adi Zolotov, Alyson Brooks, and Charles Downing from Exeter University for a critical reading of the paper. The work of M.Le D. has been supported by FAPESP (2011/24089-5) and PNPD/CAPES20132029. M.Le D. also wishes to acknowledge IFT/UNESP.

References

[1] Arena S. E., Bertin G., 2007, A&A, 463, 921

[2] Ascasibar Y., Yepes G., Gottlöber S., 2004, MNRAS, 352, 1109

[3] Ascasibar, Y., Hoffman, Y., Gottlöber, S. 2007, MNRAS 376, 393

[4] Astashenok, A. V., and Del Popolo, A., 2012, Class. Quantum Grav. 29, 085014 (doi:10.1088/0264-9381/29/8/085014)

[5] Avila Reese V., Firmani C., Hernandez X., 1998, ApJ, 505, 37

[6] Avila Reese V., Firmani C., Klypin A., Kravtsov A., 1999, MNRAS, 310, 527

[7] V. Belokurov, V., ApJ 2006,, 647, L111-L114

[8] Bertschinger E., 1985, ApJS, 58, 39

[9] Blumenthal G. R., Faber S. M., Flores R., Primack J. R., 1986, ApJ, 301, 27

[10] Bovill, M. S., & Ricotti, M. 2011, ApJ, 741, 17

[11] Boylan-Kolchin, M., Bullock, J. S., Kaplinghat, M, 2011, MNRAS 415L, 40

[12] Boylan-Kolchin, Michael; Bullock, James S.; Kaplinghat, Manoj, 2012, MNRAS 422, 1203

[13] Brooks A. M., & Zolotov, A., 2012, arXiv: 1207.2468

[14] Brooks, Alyson M.; Kuhlen, Michael; Zolotov, Adi; Hooper, Dan, 2013, ApJ 765, 22 **(B13)**

[15] Buchdahl, H. A., 1970, MNRAS, 150, 1-8.

[16] Bullock, J. S., Kravtsov, A. V., & Weinberg, D. H. 2000, ApJ, 539, 517

[17] Burkert, A. 1995, ApJ, 447, L25

[18] Cardone V. F., Sereno M., 2005, A&A, 438, 545

[19] Catelan P., Theuns T., 1996, MNRAS, 282, 436

[20] Chandrasekhar, S., 1943, ApJ 97, 255

[21] Choi, J.-H., Weinberg, M. D., & Katz, N. 2009, MNRAS, 400, 1247

[22] Colin, P., Avila-Reese, V., & Valenzuela, O. 2000, ApJ, 542, 622

[23] Cole, D. R., Dehnen,W., & Wilkinson, M. I. 2011, MNRAS, 416, 1118

[24] Colpi, M., Mayer, L., & Governato, F. 1999, ApJ, 525, 720

[25] D'Onghia, E., Vogelsberger, M., Faucher-Giguere, C.-A., & Hernquist, L. 2010b, ApJ, 725, 353

[26] de Blok, W. J. G., Bosma, A., & McGaugh, S. 2003, MNRAS, 340, 657

[27] de Blok W. J. G., McGaugh S. S., Bosma A., Rubin V. C., 2001, ApJ, 552, L23

[28] De Lucia G., Helmi A., 2008, MNRAS, 391, 14

[29] Del Popolo, A., Gambera, M., 1996, A&A 308, 373

[30] Del Popolo, A., 2009, ApJ 698, 2093 **(DP09)**

[31] Del Popolo, A., 2011, JCAP 07, 014 **(DP11)**

[32] Del Popolo, A., 2010, MNRAS 408, 1808 **(DP10)**

[33] Del Popolo, A. & Kroupa, P., 2009A&A 502, 733

[34] Del Popolo, A., 2012a, MNRAS 424, 38 **(DP12a)**

[35] Del Popolo, A., 2012b, MNRAS 419, 971 **(DP12b)**

[36] Del Popolo, A., 2013, AIP Conference Proceedings 1548 , pp. 2-63

[37] Del Popolo, A., Cardone, V. F., & Belvedere, G., 2013, MNRAS 429, 1080

[38] Del Popolo, A., Pace, F., Maydaniuk, S. P., Lima, J. A. S., Jesus, J. F., 2013, Phys. Rev D, vol. 87, Issue 4, id. 043527

[39] Del Popolo, A., Pace, F., Lima, J. A. S., 2013a, MNRAS 430, 628

[40] Del Popolo, A., Pace, F., Lima, J. A. S., 2013b, IJMPD 22, 1350038

[41] Del Popolo, A., 2014, IJMPD 23, 1430005

[42] **Del Popolo, A.** *et al.***, JCAP 1404 (2014) 021**

[43] Del Popolo, A., Baltic Astronomy, 23 (2014a) 55

[44] Del Popolo, A., Hiotelis, N., JCAP 01 (2014) 047

[45] Del Popolo, A., JCAP 1407 (2014b) 019

[46] Di Cintio, A., Knebe, A., Libeskind, N. I., Brook, C., Yepes, G., Gottlöber, S., Hoffman, Y., 2013, MNRAS 431, 1220-1229

[47] Di Cintio, A., Brook, C. B., Macció, A. V., Stinson, G. S., Knebe, A., Dutton, A. A., Wadsley, J., 2014, MNRAS 437, 415

[48] Diemand, J., et al. 2008, Nature 454, 735

[49] Diemand, J., Kuhlen, M., and Madau, P., 2007, ApJ 667, 859-877

[50] Eisenstein D. J., Loeb A., 1995, ApJ, 439, 250

[51] El-Zant A. A., Hoffman Y., Primack J., Combes F., Shlosman I., 2004, ApJ, 607, L75

[52] El-Zant, A., Shlosman, I., & Hoffman, Y. 2001, ApJ, 560, 636

[53] Ferraro, R., 2012, AIP Conf. Proc. 1471, 103-110, arXiv:1204.6273v2

[54] Fillmore J. A., Goldreich P., 1984, ApJ, 281, 1

[55] Flores, R., Primack, J. R., Blumenthal, G. R., Faber, S. M., 1993, ApJ 412, 443-454

[56] Flores R. A., Primack J. R., 1994, ApJ, 427, L1

[57] Gelato, S., & Sommer-Larsen, J. 1999, MNRAS, 303, 321

[58] Gnedin O. Y., Kravtsov A. V., Klypin A. A., Nagai D., 2004, ApJ, 616, 16

[59] Gnedin, O. Y., Hernquist, L., & Ostriker, J. P. 1999, ApJ, 514, 109

[60] Gnedin, O. Y., & Ostriker, J. P. 1997, ApJ, 474, 223

[61] Gnedin, O. Y., & Ostriker, J. P., 1999, ApJ, 513, 626

[62] Goodman, J. 2000, New Astron., 5, 103

[63] Governato et al. 2010, Nature 463, 203

[64] Governato, F., Zolotov, A., Pontzen, A., Christensen, C., Oh, S. H., Brooks, A. M., Quinn, T., Shen, S., Wadsley, J., 2012, MNRAS 422, 1231

[65] Governato, F., Weisz, D., Pontzen, A., Loebman, S., Reed, D., Brooks, A. M., Behroozi, P. and Christensen, C. *et al.***, arXiv:1407.0022 [astro-ph.GA].**

[66] Gunn J. E., 1977, ApJ, 218, 592

[67] Gunn J. E., Gott J. R., 1972, ApJ, 176, 1

[68] Gustafsson M., Fairbairn M., Sommer-Larsen J., 2006, Phys. Rev. D, 74, 123

[69] Hayashi, E., Navarro, J. F., Taylor, J. E., Stadel, J., & Quinn, T. 2003, ApJ, 584, 541

[70] Henriksen, R. N., Widrow, Lawrence M., 1995, MNRAS 276, 679

[71] Henriksen, R. N., Widrow, Lawrence M., 1997, Phys. Rev. Lett., 78, 3426

[72] Henriksen, R. N., Widrow, Lawrence M., 1999, MNRAS 302, 321

[73] Henriksen, R. N., Le Delliou M., 2002, MNRAS 331, 423

[74] Hiotelis, N., Astron. Astrophys., 2002, 383, 84.

[75] Hiotelis, N., Del Popolo, A., 2013, MNRAS 436, 163

[76] Hoffman Y., Shaham J., 1985, ApJ, 297, 16

[77] Hoyle F., 1949, in Burger J. M., van der Hulst H. C., eds, IAU and International Union of Theoretical and Applied Mechanics Symposium, Problems of Cosmological Aerodynamics. IAU, Ohio, p. 195

[78] Hu W., Kravtsov A. V., 2003, ApJ, 584, 702

[79] Hu,W., Barkana, R., & Gruzinov, A. 2000, Phys. Rev. Lett., 85, 1158

[80] Inoue, Shigeki; Saitoh, Takayuki R., 2012, MNRAS 422, 1902

[81] Inoue, Shigeki; Saitoh, Takayuki R., Mon. Not. R. Astron. Soc. 418, 2527-2531 (2011)

[82] Irwin, M. J., et al. 2007, ApJ, 656, L13

[83] Kaplinghat, M., Knox, L., & Turner, M. S. 2000, Phys. Rev. Lett., 85, 3335

[84] Kazantzidis, S., Lokas, E. L., Callegari, S., Mayer, L., & Moustakas, L. A., 2011, ApJ, 726, 98

[85] Keeton C. R., 2001, ApJ, 561, 46

[86] Klypin A., Kravtsov A. V., Bullock J. S., Primack J. R., 2001, ApJ, 554, 903

[87] Klypin A., Kravtsov A. V., Valenzuela O., Prada, F., 1999, ApJ 522, 82

[88] Klypin A., Zhao H.-S., Somerville R. S., 2002, ApJ, 573, 597

[89] Klypin, A. A., Trujillo-Gomez, S., and Primack, J., 2011, ApJ 740, 102

[90] Komatsu, E., et al. 2009, ApJS, 180, 330

[91] Kravtsov, A. V., Gnedin, O. Y., & Klypin, A. A. 2004, ApJ, 609, 482

[92] Kundić , T., & Ostriker, J. P. 1995, ApJ, 438, 702

[93] Kuzio de Naray, R., Kaufmann, T., 2011, MNRAS.414.3617

[94] Li, Y.-S.; De Lucia, G. Helmi, A., 2010, MNRAS 401, 2036, arXiv:0909.1291v2

[95] Le Delliou M., Henriksen R. N., 2003, A&A, 408, 27

[96] Le Delliou M., 2008, A&A, 490, L43-L48

[97] Le Delliou M., Henriksen R. N., MacMillan, J. D., 2010, A&A, 522, A28

[98] Le Delliou M., Henriksen R. N., MacMillan, J. D., 2011a, A&A, 526, A13

[99] Le Delliou M., Henriksen R. N., MacMillan, J. D., 2011b, MNRAS 413, 1633-1642

[100] Lukic Z., Reed D., Habib S., Heitmann K., 2009, ApJ, 692, 217

[101] Ma, C-P., Boylan-Kolchin, M., 2004, PhysRevLett 93, 021301

[102] Macció, A. V., Stinson, G., Brook, C. B., Wadsley, J., Couchman, H. M. P., Shen, S., Gibson, B. K. and Quinn, T., Astrophys. J. 744 (2012) L9 [arXiv:1111.5620 [astro-ph.CO]]

[103] Madau, P., Shen, S. and Governato, F., Astrophys. J. 789 (2014) L17 [arXiv:1405.2577 [astro-ph.GA]].

[104] Madau, Piero; Diemand, Jürg; Kuhlen, Michael, 2008, ApJ 679, 1260 -

[105] Martizzi, D., Teyssier, R., Moore, B., & Wentz, T. 2012, MNRAS, 422, 3081

[106] Mashchenko, S., Couchman, H. M. P., & Wadsley, J. 2006, Nature, 442, 539

[107] Mashchenko, S., Wadsley, J., & Couchman, H. M. P. 2008, Science, 319, 174

[108] Mayer, L., Governato, F., Colpi, M., et al. 2001, ApJ, 559, 754

[109] McGaugh S. S., Schombert J. M., de Blok W. J. G., Zagursky M. J., 2010, 708, L14

[110] Milgrom, M., 1983a, ApJ 270, 365-370

[111] Milgrom, M. 1983b, ApJ 270, 371-389

[112] Mo H. J., Mao S., White S. D. M., 1998, MNRAS, 295, 319

[113] Moore B., 1994, Nat, 370, 629

[114] Moore, B., Quinn, T., Governato, F., Stadel, J., & Lake, G. 1999, MNRAS, 310, 1147

[115] Navarro J. F. et al., 2010, MNRAS, 402, 21

[116] Navarro J. F., Frenk C. S., White S. D. M., 1996, ApJ, 462, 563

[117] Navarro, J. F., Eke, V. R., & Frenk, C. S. 1996a, MNRAS, 283, L72

[118] Navarro J. F., Frenk C. S., White S. D. M., 1997, ApJ, 490, 493

[119] Newman, A. B., Treu, T., Ellis, R. S., Richard, J., Sand, D. J., 2013a, ApJ 765, 25

[120] Newman, A. B., Treu, T., Ellis, R. S., Sand, D. J., Nipoti, C., Richard, J., Jullo, E., 2013b, ApJ 765, 24

[121] Nipoti, C., Treu, T., Ciotti, L., Stavelli, M., 2004, MNRAS 355, 1119

[122] Nusser, A. 2001, MNRAS 325, 1397

[123] Oh, S-H, C. Brook, F. Governato, E. Brinks, L. Mayer,W. J. G. de Blok ,A. Brooks, F.Walter, 2010, AJ, 142, 24

[124] Oh, S-H, de Blok, W. J. G., Brinks, E., Fabian, W., Kennicutt, R. C., Jr., 2011 AJ 141, 193

[125] Okamoto, T., Gao, L., & Theuns, T. 2008, MNRAS, 390, 920

[126] Ostriker J. P., Steinhardt P., 2003, Science, 300, 1909

[127] Peebles P. J. E., 1969, ApJ, 155, 393

[128] Peebles, P. J. E. 2000, ApJ, 534, L127

[129] Peñarrubia, J., Just, A., Kroupa, P., 2004, MNRAS, 349, 747

[130] Peñarrubia, J., et al., 2010, MNRAS 406, 1290 **(P10)**

[131] Peñarrubia, J., Pontzen, A., Walker, M. G., & Koposov, S. E. 2012, ApJL, 759, L42

[132] Polisensky and Ricotti (2014), submitted to MNRAS, private communication

[133] Purcell, C. W., Zentner, A. R., 2012, JCAP 12, 007

[134] Quinn, P. J., & Goodman, J. 1986, ApJ, 309, 472

[135] Read, J. I., & Gilmore, G. 2005, MNRAS, 356, 107

[136] Ricotti, M., & Gnedin, N. Y. 2005, ApJ, 629, 259

[137] Romano-Diaz, E., Shlosman, I., Heller, C., & Hoffman, Y. 2009, ApJ, 702, 1250

[138] Romano-Diaz, E., Shlosman, I., Hoffman, Y., & Heller, C. 2008, ApJ, 685, L105

[139] Ryden B. S., 1988, ApJ, 329, 589

[140] Ryden B. S., Gunn J. E., 1987, ApJ, 318, 15

[141] Sakamoto, T., & Hasegawa, T. 2006, ApJ, 653, L29

[142] Simha, V., Weinberg, D. H., Davé, R., et al. 2012, MNRAS, 423, 3458

[143] Simon, J. D.; Geha, M., 2007, AAS 211, 2602

[144] Sommer-Larsen, J., & Dolgov, A. 2001, ApJ, 551, 608

[145] Spergel, D. N., et al. 2007 ApJS 170 377 doi:10.1086/513700

[146] Springel, V., Wang, J., Vogelsberger, M., Ludlow, A., Jenkins, A., Helmi, A., Navarro, J. F., Frenk, C. S., White, S. D. M., 2008, MNRAS 391, 1685

[147] Stadel J., Potter D., Moore B., Diemand J., Madau P., Zemp M., Kuhlen M., Quilis V., 2009, MNRAS, 398, 21

[148] Starobinsky, A. A. (1980). Physics Letters B 91: 99-102

[149] Stoehr, F., White, S. D. M., Tormen, G., & Springel, V. 2002, MNRAS, 335, L84

[150] Strigari, L. E., Bullock, J. S., Kaplinghat, M., Diemand, J., Kuhlen, M., Madau, P., 2007, ApJ 669, 676

[151] Taylor, J. E., Babul, A., 2001, ApJ 559:716-735

[152] Treu T., Koopmans L. V. E., 2002, ApJ, 575, 87

[153] van den Bosch F. C., Burkert A., Swaters R. A., 2001, MNRAS, 326, 1205 (VBS)

[154] van den Bosch, F. C., Lewis, G. F., Lake, G., & Stadel, J. 1999, ApJ, 515, 50

[155] Vera-Ciro, C. A., Helmi, A. Starkenburg, E., Breddels, M. A., 2013, MNRAS 428, 1696

[156] Vitvitska M., Klypin A. A., Kravtsov A. V., Wechsler R. H., Primack J. R., Bullock J. S., 2002, ApJ, 581, 799

[157] Wang, J., Frenk, C. S., Navarro, J. F., Gao, L., Sawala, T., 2012, MNRAS 424, 2715

[158] Weinberg, S., Rev. Mod. Phys., 1989, 61, 1

[159] Wetzel, A. R., & White, M. 2010, MNRAS, 403, 1072

[160] White M., 2001, A&A, 367, 27

[161] White S. D. M., 1984, ApJ, 286, 38

[162] White S. D. M., Frenk C. S., 1991, ApJ, 379, 52

[163] White S. D. M., Rees M. J., 1978, MNRAS, 183, 341

[164] Williams, L. L. R., Babul, A., & Dalcanton, J. J. 2004, ApJ, 604, 18

[165] Willman, B., et al. 2005a, ApJ, 626, L85

[166] Zentner, A. R., & Bullock, J. S. 2003, ApJ, 598, 49

[167] Zolotov, A., Brooks, A. M., Willman, B., Governato, F., Pontzen, A., Christensen, C., Dekel, A., Quinn, T., Shen, S., Wadsley, J., 2012, ApJ 761, 71 **(Z12)**

[168] Zucker, D. B., et al. 2006a, ApJ, 643, L103

A Core formation model

The **cusp to core transformation model used in the following** was already described in DP09, and also in DP12a, b. Here, we give a summary.

The DP09 model is an improvement to the spherical infall models (SIM) already discussed by several authors (Gunn & Gott 1972; Fillmore & Goldreich 1984; Bertschinger 1985; Hoffman & Shaham 1985; Ryden & Gunn 1987; Henriksen & Widrow 1995, 1997, 1999; Henriksen & Le Delliou 2002; Le Delliou & Henriksen 2003; Le Delliou 2008; Ascasibar, Yepes & Gottlöber 2004; Williams, Babul & Dalcanton 2004; Le Delliou, Henriksen & MacMillan 2010, 2011a, 2011b)[11].

Previous authors studied modifications in the basic SIM of Gunn & Gott (1972) by introducing one effect at a time, such as a) "random angular momentum" (e.g., Williams, Babul & Dalcanton 2004), b) adiabatic contraction (e.g., Blumenthal et al. 1986; Gnedin et al. 2004; Klypin, Zhao, and Somerville 2002; Gustafsson et al. 2006), or c) dynamical friction of DM and stellar clumps on the halo (El-Zant et al. 2001, 2004; Romano-Diaz et al. 2008). In contrast, our model takes into account simultaneously all those effects (random angular momentum, adiabatic contraction, dynamical friction), and more (ordered angular momentum, gas cooling, star formation), as can be seen in the following.

In the SIM, a spherical perturbation is divided into spherical shells and its evolution followed in time from the initial radius x_i to the maximum expansion, x_m (called turn-around).

After turn-around, the shells collapse, crossing each other ("shell-crossing"). As a result the energy no longer remains an integral of motion. An adiabatic invariant is introduced to handle shell-crossing (Gunn 1977; Fillmore & Goldreich 1984), allowing to calculate the density profile

$$\rho(x) = \frac{\rho_{ta}(x_m)}{f(x_i)^3}\left[1 + \frac{d\ln f(x_i)}{d\ln g(x_i)}\right]^{-1}, \tag{A.1}$$

where $f(x_i) = x_i/x_m$ is the collapse factor, and the turn-around radius of a shell, x_m, is a monotonically increasing function of x_i, given by

$$x_m = g(x_i) = x_i \frac{1+\overline{\delta}_i}{\overline{\delta}_i - (\Omega_i^{-1} - 1)}, \tag{A.2}$$

being $\overline{\delta}_i$ the **initial average overdensity** inside the shell (see Appendix A of DP09).

In our model, we consider systems with DM and baryons. The way in which they were introduced, and how we fixed their distribution in our study was discussed in Appendix E of DP09.

The **baryonic** fraction was fixed in the same fashion as in McGaugh et al. (2010). The detected baryonic fraction, f_d, is defined by

$$f_d = (M_b/M_{500})/f_b = F_b/f_b, \tag{A.3}$$

where $F_b = M_b/M_{500}$ is the actual baryonic fraction and $f_b = 0.17 \pm 0.01$ (Komatsu et al. 2009) is the universal **baryonic** fraction.

[11] For dark energy implementation in the spherical collapse, see Del Popolo, Pace, & Lima 2013; Del Popolo, Pace, & Lima 2013a, b.; Del Popolo et al. 2013.

The virial mass, M_{vir}, is converted to M_{500}[12], using the method from White (2001), Hu & Kravtsov (2003), and Lukic et al. (2009).

During the evolution of the perturbation and its collapse, a random angular momentum $j(r,\nu)_{rand}$, is generated from random velocities (Ryden & Gunn 1987). Usually, in SIM papers taking angular momentum into account, the so-called "random angular momentum" is the only one considered (Nusser 2001, Hiotelis 2002; Le Delliou & Henriksen, 2003; Ascasibar, Yepes & Gottlöber 2004), frequently assigned at turn-around as

$$j_{rand} = j_* \propto \sqrt{GMr_m}, \tag{A.5}$$

or obtained by the random inner motions of the proto-structure (Ryden & Gunn 1987; Avila-Reese et al. 1998; Williams et al. 2004; Del Popolo & Kroupa 2009). Instead of directly assigning j_{rand}, one can express it in terms of the ratio of pericentric, r_{peri}, to apocentric, r_{apo}, radii. That ratio, $e = \left(\frac{r_{peri}}{r_{apo}}\right)$ (Avila-Reese et al. 1998), is constant, and approximately equal to 0.2 in N-body simulations[13]. A more detailed analysis shows that particle orbits tend to become more radial when they reach the turn-around radius. Moreover, eccentricity depends **on** the dynamical state of the system, so that

$$e(r_{max}) \simeq 0.8(r_{max}/r_{ta})^{0.1}, \tag{A.6}$$

for $r_{max} < 0.1r_{ta}$, (Ascasibar, Yepes & Gottlöber 2004). Random angular momentum is modeled here through the Avila-Reese et al. (1998) method with the Ascasibar, Yepes & Gottlöber (2004) **model.**

The other form of angular momentum**, coined the "ordered angular momentum",** $h(r,\nu)$[14]**, is** produced by the tidal torque of large-scale structures on the proto-structure (Hoyle 1953; Peebles 1969; White 1984; Ryden 1988; Eisenstein & Loeb 1995; Catelan & Theuns 1996). The total specific angular momentum, $h(r,\nu)$, is obtained by integrating the tidal torques, $\tau(r)$, over time (e.g., Ryden 1988, Eq. 35). It is common to express the total angular momentum in terms of the spin parameter. If the system is constituted of DM and baryons, the baryonic (resp. DM) spin parameter is given by

$$\lambda_{gas(DM)} = \frac{L_{gas(DM)}}{M_{gas(DM)}[2G(M_{gas}+M_{DM})r_{vir}^{1/2}]}, \tag{A.7}$$

$M_{gas(DM)}$ being the gas (resp. DM) mass inside, r_{vir}, the virial radius, and $L_{gas(DM)}$ is the angular momentum of gas (resp. DM). The λ parameter distribution is well described by a lognormal distribution (e.g. Vivitska et al. 2002). The way dynamical friction is taken into account is described in Appendix D of DP09, and its effects on structure formation is

[12]Structures are usually labeled by the their density contrast with respect to the critical density, ρ_c. The mass in a given radius encompassing the overdensity Δ is given by

$$M_\Delta = \frac{4\pi}{3}\Delta\rho_c R_\Delta^3, \tag{A.4}$$

M_{500} is the mass enclosed in R_{500}, defining the radius within which the mean structure overdensity is 500 times the critical density ρ_c.

[13]A value $e \simeq 0.2$ produces density profiles close to the NFW model. In Avila-Reese et al. (1998, 1999) it was fixed at 0.3.

[14]The peak height ν is defined as $\nu = \delta(0)/\sigma$, where $\delta(0)$ is the central overdensity value, and σ is the density field mass variance (Eq. B12 in DP09; Del Popolo 1996).

calculated, following DP09, by introducing the dynamical friction force in the equation of motion (Eq. A14 of DP09).

A fundamental **process** in galaxy formation is adiabatic contraction (AC) of DM haloes, produced by baryon condensation in the proto-structure center. AC produces a steepening of the DM density profile (Blumenthal et al. 1986; Gnedin et al. 2004; Gustafson et al. 2006) **from baryon dissipative cooling and their collapse to the proto-structure center. This gives** rise to a final baryonic mass distribution $M_b(r) = M_* + M_{gas}$, where **the gas and stars masses are** M_{gas} **and** M_* **respectively.** Dark matter particles initially located at radius r_i move to a new radius $r < r_i$, characterized by (Ryden 1988; Flores et al. 1993)

$$r_i M_i(r_i) = r\left[M_b(r) + M_{dm}(r)\right], \tag{A.8}$$

where M_{dm} is the final distribution of DM halo particles, and $M_i(r_i)$ the initial total mass distribution, and M_b, as reported, the final baryonic mass distribution. If the halo particles orbits do not cross, we have

$$M_{dm}(r) = (1 - F_b)M_i(r_i). \tag{A.9}$$

Once $M_i(r_i)$ and $M_b(r)$ are given, Eqs. (A.8), (A.9) can be iteratively solved to find the distribution of halo particles. It is usually assumed that the density profile of DM and baryons **are** the same (Mo et al. 1998; Keeton 2001; Treu & Koopmans 2002; Cardone & Sereno 2005), given by **an** NFW profile. The final distribution of baryons is assumed to be a disc (for spiral galaxies) (Blumenthal et al. 1986; Flores et al. 1993; Mo et al. 1998; Klypin et al. 2002; Cardone & Sereno 2005)[15].

The previous model was improved following Gnedin et al. (2004), who showed that numerical simulation results are better reproduced if one assumes the conservation of the product of the mass inside the orbit-averaged radius with the radius itself

$$M(\bar{r})r = \text{const.} \tag{A.10}$$

where the orbit-averaged radius is

$$\bar{r} = \frac{2}{T_r}\int_{r_{peri}}^{r_{apo}} r\,\frac{dr}{v_r}, \tag{A.11}$$

and T_r is the radial period[16].

The previous model does not **include** exchange of angular momentum **between** baryons and DM. This is a good approximation in the early phase of the structure's formation, when baryons' density is an order of magnitude smaller than DM's. However, when baryon density increase because of the collapse, the approximation is no longer valid. Baryon density increase acts as a coupling process between DM and baryons (Klypin et al. 2001; Klypin, Zhao, and Somerville 2002). Excitation of spiral waves and/or the presence of bar-like modes can give rise to a non-axisymmetric component. The coupling effect is very powerful in the last period of structure formation, with a reduction of DM density by a factor of ten (Klypin, Zhao, & Somerville 2002; DP09; DP12a, b).

[15]In DP09, the final baryonic distribution of typical spiral galaxies (e.g., MW, and M31) was determined using the Klypin et al. (2002) model (see their subsection 2.1).

[16]Gnedin et al. (2004) used $M(\bar{r})r$ = const instead of $M(\bar{r})\bar{r}$ = const because the former is a better approximation to their simulations result.

Similarly to other semi-analytical models and following the philosophy of the works from White & Rees (1978) and White & Frenk (1991), we include other important physical processes such as gas cooling, and star formation, as described below.

The structure's formation in our model can be summarized as follows. Galaxy formation starts with the proto-structure in its linear phase, containing DM and gas. In our model the baryons are initially in the form of a diffuse gas, with the baryonic fraction previously discussed. In order to follow the structure formation, we divide the proto-structure into mass shells, made of DM and baryons. The proto-structure evolution is followed in the expansion phase, until turn-around, and through the subsequent collapse by means of the SIM. As is known, DM collapse earlier than baryons to form the potential wells in which baryons fall, and are subject to radiative processes with the formation of clumps. Those clumps collapse to the halo center, condensing into stars, as described in Li et al. (2010) (Sect. 2.2.2, 2.2.3) and De Lucia & Helmi (2008), respectively. During the baryons infall phase, DM is compressed (AC). At this epoch, the density profile of the proto-structure steepens. In their travel towards the center, baryons clumps are subject to DF from the less massive DM particles. This produces a predominant motion of DM particles outwards. The effect of this mechanism is amplified by the angular momentum, acquired by the proto-structure through tidal torques (ordered angular momentum), and by random angular momentum. The cuspy profile is flattened to a cored one.

Our model is in agreement with **other papers in which exchange of energy and angular momentum from baryons clumps to DM through DF is responsible for flattening the density profile** (El-Zant et al. 2001, 2004; Ma & Boylan-Kolchin 2004; Nipoti et al. 2004; Romano-Diaz et al. 2008, 2009; DP09; Cole et al. 2011; Inoue & Saitoh 2011). It is **capable of dealing** with the baryonic processes shaping the inner structure of galaxies (and clusters). It was able to predict the correct shape of the density profiles of galaxies (DP09; Del Popolo & Kroupa 2009; DP12b), and clusters (DP12a), in advance of SPH simulations (e.g., Governato et al. 2010, 2012; Martizzi et al. 2012), as well as correlations among several quantities in clusters of galaxies (DP12a), later observed in Newman et al. (2013a,b). The model also predicts correctly that the inner slope of the density profiles depends on the halo mass (DP10, DP11), which was later seen in the SPH simulations of Di Cintio et al. (2013, 2014).

B Dynamics of the satellites.

In the following, we discuss a semi-analytic model that follows the substructure evolution within DM haloes. It takes into account the effects of DF, tidal loss and tidal heating. The model is basically the TB01 model with small changes coming from a similar model by P10.

Each satellite is represented by a spherically symmetric subhalo, whose structure is time dependent. At a time t, the satellite's state is specified by the form of the density distribution, from a chosen initial condition[17], by the mass bound to it, and by the heating experienced in time. For the determination of the satellite's orbit, we ignore its spatial extent and we solve its equation of motion in the potential of the host halo.

At each time step, the equations solved are:

$$\ddot{\mathbf{r}} = \mathbf{f}_h + \mathbf{f}_d + \mathbf{f}_{\rm df}; \tag{B.1}$$

[17]The initial density profile of the satellites is given by Appendix A.

In Eq. (B.1), the term $\mathbf{f}_h = -GM(<r)/r^2$ is the force due to the host halo, where

$$M(<r) = 4\pi \int_0^r \rho(r')r'^2 dr'; \tag{B.2}$$

and the density $\rho(r)$ is given by a NFW[18] profile with parameters $R_{\rm vir} = 258$ kpc, $r_s = 21.5$ kpc, $M_{\rm vir} = 10^{12} M_\odot$, and $\Delta_v = 101$ (Klypin et al. 2002; Peñarrubia et al. 2010). The term $\mathbf{f}_{\rm d}$ is the force produced by the baryonic disc. While in Peñarrubia et al. (2010) it is approximated by means of a Miyamoto-Nagai (1975) model, in Klypin et al. (2002) a double-exponential disc is used. We select the exponential disc applied in TB01, defined by the density

$$\rho_{\rm d}(r) = \frac{M_{\rm d}}{4\pi R_{\rm d}^2 z_0} exp(-\frac{R}{R_{\rm d}}) sech^2(\frac{z}{z_0}) \tag{B.3}$$

with $M_{\rm d} = 5.6 \times 10^{10} M_\odot$, $r_{\rm d} = 3.5$ kpc, and $z_0 = 700$ kpc. In this study, we neglect the bulge (similarly to P10), since the disc has a much larger mass than the bulge, and presents a steep vertical density gradient. **That gradient is 10 times larger than for the bulge or the halo, resulting in satellite heating at disc crossing 100 times larger than from the other components.**

B.1 Dynamical friction

The term $\mathbf{f}_{\rm df}$ is the dynamical friction force on the satellites due to the DM particles moving around the host. Dynamical friction is approximated through Chandrasekhar's formula (Chandrasekhar 1943) which is sufficiently accurate if one can consider the so called "Coulomb logarithm" as a free parameter, fixed through simulations (e.g., van den Bosch et al. 1999).

Chandrasekhar's formula, in our case is given by

$$\mathbf{f}_{\rm df} = \mathbf{f}_{\rm df,disc} + \mathbf{f}_{\rm df,halo} = -4\pi G^2 M_{sat}^2 \sum_{i=h,d} \rho_i(r) F(<v_{\rm rel,i}) \ln\Lambda_i \frac{\mathbf{v}_{\rm rel,i}}{v_{\rm rel,i}^3}. \tag{B.4}$$

having divided the potential into the halo and disc components. M_{sat} is the satellite mass, $\mathbf{r}$ its position, and $\ln\Lambda_h$ and $\ln\Lambda_d$ are the Coulomb logarithms of the halo and disc components, respectively. If $\mathbf{v}_{sat}$ indicates the velocity vector of the satellite, then $\mathbf{v}_{\rm rel,h} = \mathbf{v}_{sat}$ is the satellite's relative velocity with respect to the halo, while $\mathbf{v}_{\rm rel,d} = \mathbf{v}_{sat} - \mathbf{v}_{d,\phi}$ the relative velocity with respect to the disc, while the term $v_{d,\phi}^2 = R|f_d(Z=0)|$ is the circular velocity of the disc measured on the plane of the galaxy. The velocity distribution, $F(v)$, is assumed to be isotropic and Maxwellian, for simplicity

$$F(<v_{\rm rel,i}) = {\rm erf}(X_i) - \frac{2X_i}{\sqrt{\pi}} \exp[-X_i^2]; \tag{B.5}$$

where the term $X_i = |v_{\rm rel,i}|/\sqrt{2}\sigma_i$ is the one-dimensional velocity dispersion[19].

Chandrasekhar's formula was calculated for a massive point particle, but several authors showed that it can be applied to calculate the drag force on an extended satellite by adjusting appropriately the Coulomb logarithms (e.g., Colpi, Mayer & Governato 1999). Their choice

[18] We recall that the NFW profile is given by $\rho(r) = \frac{\rho_s}{r/r_s(1+r/r_s)^2} = \frac{\rho_c \delta_v}{r/r_s(1+r/r_s)^2}$, where $\delta_v = \frac{\Delta_v}{3}\frac{c^3}{\log(1+c)-c/(1+c)}$ and ρ_c is the critical density. The scale radius r_s, and ρ_s depend on the formation epoch and are correlated with the virial radius of the halo, $R_{\rm vir}$, through the concentration parameter $c = R_{\rm vir}/r_s$.

[19] The velocity dispersion is defined as $\sigma_i(r) \equiv 1/\rho_i(r) \int_\infty^r \rho_i(r')[f_h(r') + f_d(r')]dr'$.

is not trivial. Usually Λ is defined as $\Lambda = b_{max}/b_{min}$, where b_{max} is set to the typical scale of the system, and $b_{min} \equiv G(M_{\rm sat} + m)/V^2$, m being the mass of the background particles and V the typical velocity of the encounter, is the minimum impact parameter. A different definition is used for an extended satellite (Quinn & Goodman 1986).

The uncertainty in Λ_d and Λ_h directly reflects on that of the orbital decay rates, since the latters depend on the values of the Coulomb logarithms. A way to reduce such discrepancy is to treat $\ln\Lambda_h$ and $\ln\Lambda_d$ as free parameters. The self-consistent value of the Coulomb logarithm best fitting N-body orbits is $\ln\Lambda_h = 2.1$ (Peñarrubia, Just & Kroupa 2004; Arena & Bertin 2007), while TB01 and P10 adopt $\ln\Lambda_d = 0.5$. One should also make a correction to the expression for the disc friction, since the model assumed a constant satellite **wake**, and this approximation could reveal incorrect if the background density changes over small scales (e.g., when the satellite is **in** the disc plane). This can be corrected by smoothing the disc density (see Sec. 2.2.1 of TB01).

B.2 Mass loss

A finite size satellite moving through the host galaxy is expected to loose mass because of tidal stripping. The mass decrease of the satellite affects its dynamic, since the dynamical friction force expression contains $M^2_{\rm sat}$. It is clear that we need to estimate the mass loss in order to correctly describe the satellite motion. The loss of mass is due to the action of tidal forces. We distinguish two model behaviours: if the system is "slowly varying", we consider the material outside a limiting radius, dubbed "tidal radius", to be stripped, while if the system is "rapidly varying", the satellite material will be heated.

In the first case, one estimates the tidal radius as the distance, measured from the centre of the satellite, where the tidal force balances the satellite's self-gravity. In the case of satellites on circular orbits, the tidal radius is given by

$$R_t \approx \left(\frac{GM_{sat}}{\omega^2 - {\rm d}^2\Phi_{\rm h}/{\rm d}r^2}\right)^{1/3}; \tag{B.6}$$

(King 1962), where, as before, M_{sat} is the mass of the satellite ω is its angular velocity, and Φ_h is the host halo potential. Eq. (B.6) is valid if $M_{sat} << M_h$, $R_t << R_{system}$, and the satellite is corotating at ω. Eq. (B.6) describes a steady state loss of mass, while the mass changes on a general orbit should depend on the orbital period. One then assumes that mass beyond the tidal radius is lost in an orbital period.

The calculation of ${\rm d}^2\Phi_h/{\rm d}r^2$ is performed averaging over the asphericity of the potential originated by the disc component, as follows

$$\frac{{\rm d}^2\Phi_h}{{\rm d}r^2} = \frac{\rm d}{{\rm d}r}\left(\frac{-GM(<r)}{r^2}\right). \tag{B.7}$$

In real systems, satellites are not spherical and do not move inside spherically symmetric potentials. In such cases, Eq. (B.6) can be used to define an instantaneous tidal radius.

The stripping condition can be written in terms of the densities as,

$$\overline{\rho}_{\rm sat}(<R_{\rm t}) = \xi\overline{\rho}_{\rm gal}(<r)\,. \tag{B.8}$$

The previous equation localizes the tidal limit at the radius beyond which the satellite mean density, $\overline{\rho}_{\rm sat}$, is larger by a factor ξ than the average galaxy density inside that radius

r, where

$$\xi \equiv \frac{\overline{\rho}_{\rm sat}(< R_{\rm t})}{\overline{\rho}_{\rm gal}(< r)} = \left(\frac{r^3}{GM(< r)}\right)\left(\omega^2 - \frac{{\rm d}^2\Phi_h}{{\rm d}r^2}\right) \tag{B.9}$$

being ω the instantaneous angular velocity of the satellite and ω_c is the angular velocity of a circular orbit of radius r.

From the previous discussion, we can define an algorithm to calculate stripping.
1) We divide the orbital path of the satellite in discrete sections, and calculate the tidal radius through Eq. (B.8).
2) A fraction $\Delta t/t_{orb}$[20], of the material outside the virial radius will be removed.
3) Whereas in TB01, the satellite was considered disrupted when the tidal radius was smaller than the profile core radius, in our case, we define some other disruption criteria in Sect. 2.3.

B.3 Tidal Heating

As previously discussed, in the case of a rapidly varying gravitational potential, shocks are produced which result in changes in the satellite structure and give rise to an acceleration of the mass loss (e.g., Gnedin & Ostriker 1997, 1999; Gnedin, Hernquist & Ostriker 1999). A simple first order correction for tidal heating can be obtained as follows. Rapid shocks are identified by comparing the orbital period of the satellite, $t_{\rm orb,sat}$[21], with the disc shock timescale, $t_{\rm shock,d} = Z/V_{Z,\rm sat}$. If $t_{\rm shock,d} < t_{\rm orb,sat}$ the satellite is heated. We then calculate the change in energy, and the subsequent mass loss in the satellite. The energy change is obtained adopting the impulse approximation (Gnedin, Hernquist, & Ostriker 1999), which yields the velocity change produced by the tidal field in the encounter, relative to the center of the satellite.

This velocity change produced in an encounter of duration t, for an element of unit mass located at $\mathbf{x}$ with respect to the center of the satellite, writes

$$\Delta\mathbf{V} = \int_0^t \mathbf{A}_{\rm tid}(t')dt', \tag{B.10}$$

where the term $\mathbf{A}_{\rm tid}$ is the tidal acceleration.

The first order change in energy is given by

$$\Delta E_1(t) = W_{\rm tid}(t) = \frac{1}{2}\Delta V^2 \tag{B.11}$$

We divide the shock in n time steps of length Δt and suppose that the satellite is sufficiently small so that the tidal acceleration can be expressed in terms of the gradient of the gravitational acceleration produced by the external potential, $\mathbf{g}$. We then average the change of energy on a sphere of radius r, in a time step, as

$$\begin{aligned}\Delta W_{\rm tid}(t_n \rightarrow t_{n+1}) \\ = \frac{1}{6}\, r^2\, \Delta t^2 \Bigg[2\, g_{a,b}(t_n) \sum_{i=0}^{n-1} g_{a,b}(t_i) \\ + \quad g_{a,b}(t_n) g_{a,b}(t_n) \Bigg]\end{aligned} \tag{B.12}$$

[20] Δt is the timestep, while $t_{orb} = 2\pi/\omega$ is the orbital period, which is assumed to be the typical time-scale for the mass loss of the satellite.

[21] $t_{\rm orb,sat} = 2\pi r_{\rm h}/V_c(r_{\rm h})$ is the satellite orbital period at its half-mass radius, r_h.

where $g_{a,b} = \partial g_a / \partial x_b$ is evaluated at $\mathbf{x} = 0$.

The impulse approximation, upon which the calculation of Eq. (B.12) is based, breaks down in the central part of the satellite where the dynamical time-scales can be comparable to, or even shorter than, the duration of the shock. When this happens the shock effects are significantly reduced.

This is taken into account through a first-order adiabatic correction (Gnedin & Ostriker (Gnedin & Ostriker 1999)

$$\Delta E_1 = A_1(x) \Delta E_{1,\mathrm{imp}} \ , \tag{B.13}$$

where $x = t_{\mathrm{shock}}/t_{\mathrm{orb,sat}}$ is the adiabatic parameter, and $A_1(x) = (1+x^2)^{-\beta}$, with $\beta = 5/2$ (Gnedin & Ostriker 1999).

Another correction required is connected to the satellite internal dispersion velocity, which is altered by heating (Kundić & Ostriker 1995). We start by computing the energy changes at first-order and further take into account the higher order effects through the heating coefficient, ϵ_{h}, as

$$\Delta E = \epsilon_{\mathrm{h}} \Delta E_1 = \epsilon_{\mathrm{h}} A_1(x) \Delta E_{1,imp} = \epsilon_{\mathrm{h}} A_1(x) \delta W_{tid}. \tag{B.14}$$

Gnedin & Ostriker (1997) estimated $\epsilon_{\mathrm{h}} \simeq 7/3$.

In this paper, we follow TB01 in adopting the value $\epsilon_{\mathrm{h}} = 3$.

Practical determination of the effect of heating on the satellite leads us to assume for each mass element that its potential energy is proportional to its total energy. We note that shell crossing is not taken into account by the mass distribution changes.

Consequently, we write that a mass element will have a total energy $E(r)$ proportional to $-1/r$, and a radius change $\Delta r \propto \Delta E(r)\ r^2$.

Inside radius r the mean density will change as

$$\Delta \overline{\rho}_r = \ \Delta \left(\frac{3M(<r)}{4\pi r^3} \right) \ \propto -\frac{\Delta r}{r^4} \propto -\frac{\Delta E(r)}{r^2} \ . \tag{B.15}$$

The previous equation shows how the bound mass density in the satellite can decrease because of heating, with the results of an acceleration of the mass loss. The decrease in density can correspond to, either an increase of the velocity dispersion in, or an expansion of, the satellite. In any case, it gives rise to the same change in the bound mass.

We can calculate the density change due to tidal heating, at a radius r as a function of time. Applying then the equation for tidal stripping, (Eq. B.8), to the heated density we can estimate the quantity of mass lost.

In the calculation, we smoothed the disc mass in the vertical direction, as already mentioned, over twice the disc scale height. We assume the velocity dispersion of the disc to read as

$$\sigma_{\mathrm{h}} = (V_{\mathrm{c,h}}^2)^{1/2}/\sqrt{2},$$

and

$$\sigma_{\mathrm{d}} = V_{\mathrm{c,d}}/\sqrt{2} = \sigma_{\mathrm{o}} \exp(-R/R_{\mathrm{o}})$$

where $V_{\mathrm{c,h}}$, is the circular velocity of the halo, and $V_{\mathrm{c,d}}$ that of the disc. σ_{o} is set to 143 km/s and R_{o} to 7kpc (namely $2\,R_{\mathrm{d}}$), in agreement with Velasquez & White (1999).

The model depends on three parameters: $\ln \Lambda_{\mathrm{h}}$ (strongest dependence), ϵ_{h} (weaker than the previous), and $\ln \Lambda_{\mathrm{d}}$ (weak dependence). To evaluate the sensitivity of the results to parameter variations, 20% changes in the second parameter (ϵ_{h}) were issued: even with such modulations, only slight changes to the results were produced.